INNOVATIVE FOUNDATION ALTERNATIVE INSPIRED FROM TREE ROOTS

by

Macie Larranaga

A thesis

submitted in partial fulfilment

of the requirements for the degree of

Master of Science in Civil Engineering

Boise State University

August 2022

BOISE STATE UNIVERSITY GRADUATE COLLEGE

DEFENSE COMMITTEE AND FINAL READING APPROVALS

of the thesis submitted by

Macie Larranaga

Thesis Title: Innovative Foundation Alterative Inspired From Tree Roots

Date of Final Oral Examination: 17 June 2022

The following individuals read and discussed the thesis submitted by student Macie Larranaga, and they evaluated the student's presentation and response to questions during the final oral examination. They found that the student passed the final oral examination.

Bhaskar Chittoori, Ph.D., P.E.   Chair, Supervisory Committee

Nick Hudyma, Ph.D., P.E.   Member, Supervisory Committee

Robert Hamilton, Ph.D., P.E.   Member, Supervisory Committee

The final reading approval of the thesis or dissertation was granted by Bhaskar Chittoori, Ph.D., P.E., Chair of the Supervisory Committee. The thesis was approved by the Graduate College.

DEDICATION

For my family – Fernand Larranaga Jr., Victoria Larranaga, Erica Larranaga,

Riley Larranaga, Fernand Larranaga III (Tre)

ACKNOWLEDGEMENTS

This thesis, which would not be possible without the grace of God, is dedicated to my family. To my mother who always told me I could achieve anything I put my mind to, you gifted me with a love of learning. To my father who always took his little girl with him to job sites, you gifted me with a love of building. To my sister, Erica, who gifted me with laughter. To my brother, Riley, whose passion has fueled my entire life and has always been my unwavering support. To my brother, Tre, who gifted me with being a big sister and I completed my masters to show him he can do anything he puts his mind to.

I'd like to thank my advisor, Dr. Bhaskar Chittoori, for all his support and encouragement during my undergraduate and graduate time at Boise State University. His passion for geotechnical engineering and research is infectious and has helped me find my own passion in this field. I'd also like to thank him for believing in my abilities and gifting me this research. It has become a passion for me over these past two years.

ABSTRACT

It is not easy to find a more efficient foundation system than the roots of a tree. Trees create a vast three-dimensional network of roots to support and anchor the critical above-ground trunks, leaves, and limbs. In this work, investigations are made for the feasibility of imitating such a technique and creating similar networks to support civil infrastructure, particularly those subjected to moment loads such as traffic signal posts. Some of the raised questions were: Is it feasible to have a shallow tree root-based foundation system to provide the same capacities as conventional foundation alternatives? If this is feasible: What would be the ideal depth of the Root Foundation System? How far should the roots extend to provide comparable support to a conventional deep foundation system? What diameter should the root bulb of the configuration be? How far should a vertical shaft extend into the ground?

Hence, the main objective of this research is to identify and test the most effective Root Foundation System geometric configurations that can provide a similar capacity as a conventional foundation for traffic signal posts. Finite element model simulations on 54 different root-based foundation models show potential for replacing the conventional drilled shaft foundation for traffic signal posts. The conventional foundation was also modeled and produced a 0.528 mm deflection. Whereas some of the best performing root foundation models achieved 0.23 mm. By comparing the resulting deflection of the conventional foundation model to the deflection of the root foundation models, the best performing root foundation models were constructed from steel and physically tested.

The root foundation models were then calibrated to predict the performance of root foundation models. Results show that the RFSs with half the length and diameter of conventional deep foundations (for traffic signal poles) were able to provide more than four times the lateral load capacity compared to the control sections. This shows that RFSs have excellent potential to replace the conventional deep foundation alternatives used to support traffic signal posts. The economic and environmental impacts due to the root-inspired foundation systems could be tremendous owing to the reductions in the material requirements.

TABLE OF CONTENTS

LIST OF TABLES

LIST OF FIGURES

CHAPTER ONE: INTRODUCTION AND BACKGROUND

Introducing Root Foundation Systems (RFS)

Tall slender lightweight structures subjected to large overturning loads, such as sign structures, towers, or windmills, are commonly supported by conventional foundations such as mats, pile groups, and/or piled-rafts. These foundations are generally uneconomical as they are typically overdesigned, expensive, and have negative environmental impacts. A study conducted on the effects freshly poured concrete had on a nearby waterway showed the concrete caused the pH in the water to rise and fish to become distressed (Setunge et al. 2009). This is a small example of why it would be beneficial to develop an efficient foundation configuration that uses less materials and minimizes environmental and economic impacts. To develop such efficient foundation systems, one does not have to look further than tree roots. It is difficult to find a more efficient foundation system than the roots of a tree. Trees create vast networks of roots to support and anchor the critical above ground trunks, leaves, and limbs. Therefore, an attempt is made here to develop a new and innovative type of foundation using biomimicry, called the root foundation system (RFS). Biomimicry is the process of applying nature's evolved strategies to solve complex human challenges (Helms et al. 2009; Mak and Shu 2004). Therefore, the hypothesis of this research is RFS's are a feasible foundation alternative that provide the same capacities as a conventional foundation while producing similar, or less, deflections. To address this hypothesis a

clear understanding of how to use biomimicry in the engineering field, tree root mechanics, and previous studies of numerical analysis of tree roots must be understood.

Imitating natural phenomenon, also known as biomimicry, is not a new concept in today's world. It has been successfully applied to build many successful innovations. Several notable examples of biomimicry are helicopters inspired from dragonfly's wings, bullet trains inspired from the shape of a king fisher's beak, underwater signal transfer mechanisms inspired from dolphin communication, and the Eastgate Centre (shopping center) inspired from termite mounds to control the temperature naturally inside the building ("The Biomimicry Institute" 2020).

Biomimicry in Civil Engineering

In the engineering field biomimicry is a relatively new concept, however recent advancements have shown it can be an extremely effective design tool. A study (Zhang et al. 2018) explored biomimicry by modeling the wheel of a tractor rotary tiller after a soil-burrowing dung beetle's foreleg end-tooth due to its special outer contour curve that has the potential of reducing soil penetration resistance and increase soil-borrowing efficiency. MALAB and CAD software were used to manufacture the protypes exact curvatures and geometric characteristics based on the scans of a dung beetle's foreleg end-tooth. The models were then produced using a CNC machining center. To verify and compare the soil and wheel tooth interaction, an Abaqus 3D model was used to analytically evaluate stresses within the soil as well as the wheel tooth face. Applied loads to the model were 200 N, 250 N, 300 N, 350 N and 400 N which resulted in a reduced resistance of 9.5%, 11%, 13%, 13.9% and 16.5%, respectively, compared to the conventional tooth wheel. These loads also resulted in an increase of volume imprinted

depression by 11%, 7.5%, 7.5%, 12.5% and 24.9%, respectively, compared to the conventional tooth wheel. The Abaqus results of the dung beetle wheel tooth saw an increase of 14.1% in stress concentrations in the penetrating stages and a reduced 11.8% stress concentration during the lifting stage. By improving the shape of a soil-digging tool the depression volume increased, and the draft force decreased which makes it the preferred design for a tractor rotary tiller machine. It was also concluded that the special outer contour curvature of the dung beetle's foreleg tooth should be implemented in the design of other soil-engaging methods in civil engineering.

Another application of biomimicry in the civil engineering field is the study of durable concrete inspired from natural material and bacteria by (Raju Aedla 2014). The idea of bacterial concrete came from natural materials and bacteria that can engage with their surroundings, react to them and heal. Specially, Bacillus subtilis JC3 and nutrients were the bacterial components added together to make a solution in which to submerge concrete samples in. This study found Bacillus subtilis JCS acts as a self-healing agent when interacting with concrete. A water absorption test, according to the ASTM C642 (82), was performed to determine the water penetration. This test along with the ASTM C1585 (20) sorptivity test, allowed them to find the absorption of the solution took 96 hours and measure the volume of permeable voids. The samples were artificially cracked and set in the bacterial solution for 7 days to study the healing. The results showed a 16% increase of 28-day compressive strength in comparison to normal concrete that did not receive a 7-day bacterial solution treatment. They attribute this increase of compressive strength to the bacteria's ability to grow filler material within the concrete voids. Bacillus subtilis JC3 also precipitates a layer of calcium carbonate, which seals voids after new

growth has occurred. They also witnessed an increased packing density and reduced capillary porosity. This study used biomimicry to prove bacterial concrete has a better resistance to exterior damages over time. These previous investigations validate the use of biomimicry in civil engineering designs with the use of finite element method and Abaqus software, as well as highlighting the importance of using biomimicry in civil engineering designs to improve upon the current methods and standards.

Background on Tree Roots

Since this research aims to use the biomimicry of tree roots to design a new foundation design method, it is important to understand how tree roots grow and the mechanics behind tree stability against wind loads. Tree root systems typically have fairly shallow foundations, typically no deeper than 2 meters, and most roots spread laterally in the top 60 centimeters of soil. Roots growing laterally are largely responsible for the structural support of a tree's foundation. While roots initially grow in a downward vertical direction, after the first 2 or 3 years of tree growth they extend laterally towards the tree's drip line in order to get the moisture and nutrients. After years of growth, lateral roots thicken toward the center bulb of roots and then taper until reaching a 2-3 meter distance from the bulb. Roots that extend the furthest from the trunk are usually very close to the surface of the soil.

Often, roots are met with obstacles in their path of growth such as buried infrastructure or natural features in the subsurface, and they are typically deflected from the obstacle and continue their growth path (Dobson 1995a). This is a small example of the strength and foundational flexibility roots possess. Since root depth, distribution, and spread depend heavily on the soil conditions they grow in, it begs the question, how

strong could root system foundations be if they are inorganically made and do not rely on soil conditions? It is upon this basis of tree root understanding that the numerical models in this research were designed and tested.

Fully matured tree root systems can be classified into three categories: heart or bulb root systems, plate root systems, and tap root systems. As explained by (Stokes and Guitard 1997a), a bulb system's roots grow horizontally and vertically from the base of the tree slowly forming a bulb. A plate system has horizontal lateral main roots where smaller, secondary vertical roots grow from these main roots. Lastly, a tap system has a main vertical root which anchors the tree in the soil with horizontal lateral secondary roots. In this research, bulb and tap root systems have been chosen to model tree root foundations due to their ability to resist lateral and moment loads.

Although tree root systems can be classified into three categories, different species of trees produce varying root structures. Two specific tree root systems have been chosen, the bulb and tap root systems, to model foundation systems. Sabal palm trees have root systems that create vast root networks withstanding up to 145 mph winds. Their root systems have a root bulb directly below the trunk of the tree that acts as an anchor and smaller roots branching from it reinforcing its foundation radiating in all directions. The tree root bulbs are typically 1.2 m to 1.5 m in diameter and 4.6 m to 6.1 m in depth, while the smaller roots typically have a diameter of 13 mm and can grow to a depth of 4.6 m to 6.1 m (Vaile and McKnight 2017). Although it is possible for the sub-roots to grow to a depth of 4.6 m to 6.1 m, most remain within the top 0.30 m to 0.91 m of the topsoil.

Redwood (giant sequoia) trees can grow up to 91.4 m (300 ft) in height with a 7.6 – 15.3 m diameter trunk. They can weigh up to 500 tons and withstand 100 mph winds due to their tap root system acting as a shallow, mat-like spread foundation. Redwoods' tap roots radiate up to 4,046.9 m² (1 acre) laterally while only reaching 3.7 – 4.5 m in depth (Welker's Grove Nursey 2021). The reliability of sabal palm and redwood root systems in extreme weather winds make them the perfect example to model bulb and tap root foundations after, respectively.

Biomimicry of Tree Root Systems

There have been previous works that have successfully modelled tree roots to solve engineering problems. In the study carried out by (Liang et al. 2017), they found that landslides caused by seismic conditions or large amounts of rainfall are partially mitigated or prevented by retaining walls, piles, or other similar traditional methods. However, they also found that the most efficient and environmentally healthy solution, is vegetation. Rather than planting vegetation and waiting months or years to see improvement, they decided to study root properties through geotechnical centrifuge modeling. The aim of their study was to produce a tree root model that can be tested multiple times in centrifuge modeling to portray a root system's spatial distribution, geometry, and mechanical properties more accurately. When studying the architecture of root systems, two types of influence zones were assigned: the critical root zone (CRZ) and the zone of rapid taper (ZRT). CRZ is approximately 1/3 – 1/2 the area that roots actually occupy and acts as a protection zone for the system. The ZRT has the dominant structural roots that make up 80% of the total root mass. The lateral roots that extend beyond the ZRT, span many meters and taper to 10-20 mm in diameter. The lateral roots

beyond the ZRT have significantly decreased strength and rigidity. Regardless of the depth smaller roots reach, the majority of a root system's biomass lies in the topsoil and root density reduces as depth increases. Root mechanical properties were defined by Young's Modulus (E) of material and moment of inertia (*I*). The ultimate tensile strength (UTS) of the roots was defined as a function of root diameter. According to Tobin, (Tobin et al. 2007), when shear loading is applied the peak strength of soil will be reached first followed by roots enhanced shear strength until they fail.

The models were 3D printed at a 1:10 scale with an acrylonitrile butadiene styrene (ABS) plastic material. Four groups of root dimensions were defined as small, medium, large and coarse as well as two different types of root functions; root clusters and straight root groups. A total of 14 tests were conducted on a large direct shear apparatus to test the elements that affect root and soil interaction and to support the centrifuge test results. Their results showed that when shear loading was applied tap root systems were able to structurally transfer the loads through the system until they reached the smaller, deeper roots which often results in them breaking off from the cluster. They also found that the reinforcement the roots provided depends on confining stresses, depth of the slip plane given to roots and the root's morphology. When straight root groups were compared with clusters, the centrifuge results showed both types improved the slope stability problem compared to that of a conventional model. This study validates the use of biomimicry to solve engineering problems, finite element modeling's ability to accurately predict tree root behavior, and the benefits of using artificial tree roots.

Another study that advanced the capabilities of using artificial roots in engineering practice was aimed at simulating the effects of plant transpiration

(Kamchoom et al. 2016a). Plant transpiration provides suction in soil which causes increased soil strength and decreased water permeability. The artificial root system was designed with a hydraulic head inside the root that could be lowered by a vacuum. These artificial roots were made with a high air-entry value (AEV) filter, due to the small pore sizes this kind of filter provides. The water pressure the vacuum generates can be maintained in the water-saturated filter, so long as the vacuum is less than the filter. The result of upward water flow from the soil, through the filter can be achieved by the lower head being inside the root. Cellulose acetate (CA) was chosen as the porous filter due to its high AEV (100 kPa) and CA has an elastic modulus of 83 MPa and a tensile strength of 31 MPa which is close to real tree root's properties.

Direct shear tests were conducted to investigate the soil-root interface friction under varying normal stresses. Three tests carried out in soil boxes that allowed drainage; one test box has an artificial root system in it, one test box had a transplanted living tree in it and the last test box was the control in which nothing was placed in it. The soil used was a compacted, completely decomposed granite (CDG). The first stage of testing, a -98 kPa constant vacuum, was applied to the artificial root box for 48 hours while the living tree box was naturally producing soil suction. The boxes were also covered to prevent moisture loss through evaporation. Soil suction was measured by three tensiometers. The second stage of testing was a simulated 100-year rain fall period and the suction was again measured over time. The results showed the artificial root system and the tree had achieved the same suction. Their results also suggested the tree root and artificial root's ability to suction was deeper than the root's themselves. Overall, it was found that artificial root systems are capable of increasing soil strength and decreasing water

permeability. Furthermore, this method could be applied to solve engineering problems such as slope instability and minimizing water transport through evapotranspirative landfill covers.

A study conducted by (Shrestha and Ravichandran 2020) investigated wind turbine towers designed with a tree root foundation system through finite element models created in a finite element software called ABAQUS. The foundations used to model root foundations were six, twelve and eighteen main roots in a root foundation system. Three-dimensional individual parts were created in ABAQUS and combined to assemble a complete model. The soil, tree bulb, main roots, sub-roots, and taproot (simulating a drilled shaft) were modeled as linear elastic materials. However, they noted that using non-linear material properties may yield better results. The roots were designed with a reinforced polymetric pile (RPP) material in mind for the root material, due to its light weight and being a more environmentally friendly material than most conventional materials used. The geometry of all these parts is very complex therefore, a 10-noded quadratic tetrahedron element (C3D10) was used to describe the model. A combination of partitioning and a fine mesh was used to analyze areas where stress concentrations were present. Analysis was completed with the initial step, geostatic step, and a loading step in order to get a full configuration of interaction and load distribution. These models were compared with additional sub-roots attached to the main roots. In their results, it was found that an increase in the number of main roots improves performance in both differential and horizontal displacement. Whereas the addition of sub-roots had an insignificant improvement in performance. Of all the models simulated, the deflection did

not exceed 0.0749 m. However, it should be noted that this study did not compare their root model's results to a conventional foundation model's result.

This root foundation idea has been explored by professionals in the biology field and should be taken into consideration. There was a study done by (Stachew et al. 2021), which discussed developing a root based foundation system for coastal areas. Using root biomechanics, they studied the effects roots have on anchorage and growth, slope stability, wave attenuation, and lateral above ground stresses. They proposed several different coastal foundation designs which combined multiple root systems that addressed adaptive soil penetration, surface texture, complex topology, hierarchical morphology, material gradients, and root growth principles. Overall, they put forth several theoretical foundation designs that can bridge the gap between biology and engineering.

A similar study was done from a biology point of view (Coder 2018), where they investigated how tree anchorage and root strength contribute to a tree's ability to resist overturning from lateral wind loads. By examining tree attributes, they were able to conclude that as a tree's diameter doubles the energy to cause failure increases by thirty. Similarly, by studying the reactions that trees and their roots' have due to force they were about to summarize the wind force present at the top of a tree as an equation:

$Wind\ Force\ at\ Tree\ Top$

$$= 0.5 \times drag\ coefficient \times air\ density \times (wind\ velocity)^2$$

$$\times projected\ frontal\ crow\ area$$

$$\times\ height\ wind\ pressure\ center\ in\ crown$$

They were able to define an equation that estimates tensile strength in roots, where the ranges are dependent on the species of tree:

$$Root\ Tensile\ Strength = (23\ to\ 64) \times (root\ diameter)^{(-0.5\ to\ -1.0)}$$

An equation to estimate the force required for failure was also developed:

$$Force = \ 3.1416 \times root\ diameter \times root\ length$$

$$\times root\ \&\ soil\ strength\ in\ friction\ \&\ cohesion$$

Their research concluded that tree anchorage is dependent on the following: shear strength, root resistance, weight of tree, root's ability to resist buckling/hinging in compression and shear, root strength in the cross section, large roots and stem base resistance, and soil moisture content must less than its plastic/liquid limit.

This research into root foundation systems must bear all these previous studies in mind. The effectiveness of applied biomimicry to enhance engineering practices has been proven through the works by (Zhang et al. 2018). By understanding the mechanics of the three tree root system categories, bulb and tap root systems have been selected as the two root systems to model after. Specifically, sabal palm root systems for bulb roots and redwoods root systems for tap roots, were chosen because of their ability to resist the similar lateral loads and moments that the root foundation systems will experience. The advancements made in using artificial roots solidify the idea that numerical modeling, backed by physical testing, can accurately predict artificial root's behavior. The previous root foundation study, by (Shrestha and Ravichandran 2020), showed great potential for root foundation systems to be implemented. However, since no conventional foundation was tested for comparison, it is difficult to say if they are a feasible alternative to conventional foundations. There was also no physical testing to back their numerical findings, therefore they have not been calibrated. This research will include the analysis of a conventional foundation and provide physical testing to back the numerical findings.

All the works related to this topic have been significant in furthering the advancement of biomimicry, the use of artificial roots and numerical modeling in civil engineering. Building on all these previous studies, the root foundation systems will be numerically modeled and physically tested accordingly.

Traffic Signal Pole Foundations

This research specifically targets traffic signal pole foundations due to them being tall structures subjected to overturning loads. A lightweight pole has been selected as the conventional foundation and this research will aim to develop a RFS that has a similar or better capacity than the current foundation in practice. According to the Ada County Highway District (ACHD), (Ada County Highway District 2018), a traffic signal pole with a 50 ft pole and a 50 ft mast arm should have a circular foundation with a 3 ft diameter and 8 ft depth. This foundation is identified in ACHD as a traffic signal foundation type C, with #4 hoops and #6 vertical rods. According to Idaho Transportation Department (ITD) approximately 2.1 cu. yds. of concrete are required.

ITD (Idaho Transportation Department (ITD) 2017) and ACHD (Ada County Highway District 2018) specifications require traffic signal pole foundations to withstand 90 mph winds. The native soil properties given in these standard drawings are; an allowable bearing pressure of 95.8 kPa (2,000 psf), allowable lateral bearing pressure of 14.4 kPa (300 psf), and a friction angle of 30 degrees. It is important to note that these are general soil parameters and not consistent throughout Ada County. Therefore, a medium dense soil will be used in this study instead.

Research Objectives and Tasks

The hypothesis of this thesis is that a root foundation system (RFS) is a feasible foundation alternative that provides the same capacities as a conventional foundation for a traffic signal pole while producing similar, or less, deflection. Several research objectives were defined to validate this hypothesis:

1. Establish the best performing RFS geometric configurations via numerical simulations.

2. Develop an experimental test setup to physically test the best performing RFS.

3. Demonstrate the effectiveness of RFS using calibrated FEM models

To accomplish these objectives, the following tasks were performed:

1. Numerically model the current conventional foundation as the control model.

2. Numerically model different RFS geometric configurations and compare to the control model.

3. 3D print the best performing RFSs and physically test them.

4. Calibrate the RFS numerical models with the physical testing data.

5. Compare and contrast results to make final recommendation.
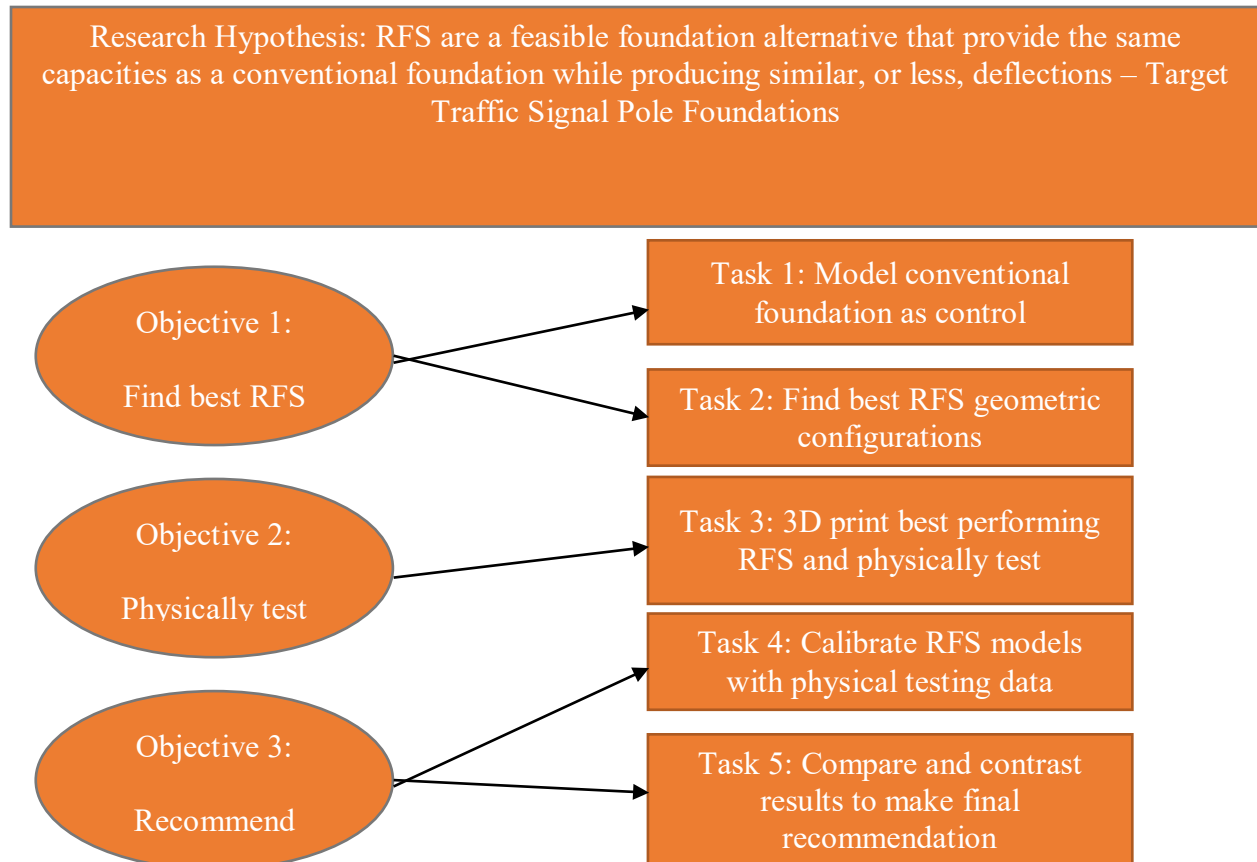
Figure 1.1.   Flow Chart of Research Work

Organization of the Thesis

This thesis consists of five chapters, three of which were prepared for publication in scientific journals and conferences.

Chapter One provides an abstract about this thesis paper, a introduction into Root Foundation Systems (RFS), a background into biomimicry and a background into tree root systems.

Chapter Two is a conference paper published in the 20th International Conference of Soil Mechanics and Geotechnical Engineering (ICSMGE) 2022. This conference paper focuses on the bulb root foundation systems of this research. It provides a literature

review into bulb root systems and biomimicry in the engineering field, as well as the preliminary modeling process and results of the twenty-seven bulb root numerical models. The best performing bulb root model showed a 58% reduction of deflection compared to a conventional foundation.

Chapter Three is a conference paper published in the GeoNiagara 2021 conference. This paper highlights the tap root foundation systems of this research. It presents a tap root and biomimicry literature review, the process and results of numerically modeling tap root foundation systems. Out of the twenty-seven different tap root models, seventeen of them showed a reduction of deflection when compared to a conventional foundation.

Chapter Four contains a journal article that is yet to be published. This paper builds off the two previously published papers, where the best performing RFS from the preliminary modelling were chosen to be scaled down and physically tested. The scaled RFS physical testing's process, results and limitations are presented. After the physical data had been collected, the numerical models were calibrated and compared. To get a full picture of RFS feasibility, full scale models were developed and calibrated to the physical testing before making final recommendations.

Finally, Chapter 5 provides a conclusion of the entire research process and findings. Final recommendations of RFS and future work has also been provided.

CHAPTER TWO: INNOVATIVE FOUNDATION ALTERNATIVE INSPIRED FROM TREE ROOTS

Abstract

It is not easy to find a more sustainably efficient foundation system than the roots of a tree. Trees create a vast three-dimensional network of roots to support and anchor the critical above-ground trunks, leaves, and limbs. In this work, we investigate the feasibility of imitating such a technique and creating similar networks to support civil infrastructure, particularly those subjected to moment loads such as traffic signal posts. Some of the raised questions were: is it feasible to have a shallow tree root-based foundation system to provide the same capacities as conventional foundation alternatives? If this is feasible: what would be the ideal depth of the Root Foundation System? How far should the roots extend, and at what angles to provide comparable support to a conventional deep foundation system? What diameter should the root bulb of the configuration be? How far should a vertical shaft extend into the ground? Hence, the main objective of this research is to identify and test the most effective Root Foundation System geometric configurations that can provide a similar capacity as a conventional foundation for traffic signal posts. Finite element model simulations on 27 different root-based foundation models showed potential for replacing the conventional drilled shaft foundation for traffic signal posts.

Introduction and Background

Tall, slender structures such as traffic signal poles are commonly supported by conventional foundations such as mats, pile groups, and pile-rafts which are typically overdesigned, expensive to construct, and have heavy environmental impacts due to their use of large amounts of raw materials such as cement and steel. Unnecessary deep foundations, such as traffic signal poles, resulting in a variety of heavy metals and toxins being introduced to the soil we build on and ecosystems depend on. With the depth of such foundations, these harmful chemicals can seep into groundwater which has a ripple effect on the life of humans and the living organisms around us. In the world we live in today, it is paramount that we decrease the impact that infrastructure has on the surrounding environment. Therefore, an attempt is made here to develop a new and innovative type of foundation using biomimicry, called the Root Foundation System (RFS).

Imitating natural phenomenon, also known as biomimicry, is the process of applying nature's tested strategies to solve complex human challenges (Mak and Shun, 2004; Helms et al., 2009). It is not a new concept in today's world. It has been successfully applied to build many successful innovations. Several notable examples of biomimicry are helicopters inspired from dragonfly's wings, bullet trains inspired from the shape of a king fisher's beak, underwater signal transfer mechanisms inspired from dolphin communication, and the Eastgate Centre (shopping center) inspired from termite mounds to control temperature naturally inside the building (Biomimicry Institute, 2020). It is a relatively very new idea in the field of geotechnical engineering to use biomimicry. Current bio-inspired geotechnics research is inspired from organisms such as worms,

ants, and termites to solve geotechnical problems in topics such as soil excavation and

penetration, soil exploration, soil–structure interaction, and mass and thermal transport in

soils (Martinez et al. 2021).

Another inspiration is tree roots. Tree root systems typically have shallow

foundations of no deeper than 2 meters, where most roots spread radially in the top 0.60

meters of soil (Dobson, 1995a). Roots growing laterally are largely responsible for the

structural support of a tree's foundation. While roots initially grow in a downward

vertical direction, after the first 2 or 3 years of tree growth, they extend laterally towards

the tree's drip line to get the moisture and nutrients they need. Roots that extend the

furthest from the trunk are usually very close to the surface of the soil. Often, roots are

met with obstacles in their path of growth, such as building foundations, rocks, etc., and

they are typically deflected from the obstacle and continue their growth path (Dobson,

1995a). This is a small example of the strength and foundational flexibility roots possess.

While root depth, distribution, and spread depend heavily on the soil conditions they

grow in, it begs the question, how strong could root system foundations be if they are

inorganically made? It is upon this basis of tree root understanding that the numerical

models in this research will be designed and tested. Sabal palm and coconut trees have

root systems that create vast root networks withstanding up to 145 mph winds. Their root

systems have a root bulb directly below the trunk of the tree that acts as an anchor and

smaller roots branching from it, reinforcing its foundation radiating in all directions

(Shruti 2019). The tree root bulbs are typically 1.2 m to 1.5 m in diameter and 4.6 m to

6.1 m in depth, while the smaller roots typically have a diameter of 13 mm and can grow

to a depth of 4.6 m to 6.1 m (Vaile and McKnight 2017). Although it is possible for the

sub-roots to grow to a depth of 4.6 m to 6.1 m, most remain within the top 0.3 m to 0.91 m to the topsoil. The reliability of sabal palm and coconut trees in extreme weather conditions makes them the perfect example to model RFSs after.

(Shrestha and Ravichandran 2020) investigated wind turbine towers designed with a foundation system inspired from sabal palm trees using finite element modeling. Foundations containing six, twelve, and eighteen main roots were modeled. The soil, tree bulb, main roots, sub-roots, and taproot (drilled shaft) were modeled as linearly elastic. However, they noted that using nonlinearities for soil may yield better results. Results showed that an increase of main roots improves performance in both differential and horizontal displacement. At the same time, the addition of sub-roots had an insignificant improvement in performance. The highest deflection among all models studied in their study was 0.0749 m.

A similar analysis was performed in this research by replacing conventional foundations for traffic signal poles with RFS. Three key variables were analyzed to find the optimum geometric configuration that could withstand the same moment and lateral load as conventional foundations can while producing a relatively similar (or less) deflection. The three key variables were bulb diameter, root length, and shaft length. Finite element modeling was employed to simulate both conventional and RFS-supported traffic signals. The details of these analyses and the corresponding results are presented in the following sections.

Numerical Modeling

Finite element modeling software Abaqus was selected for this research due to its ability to model and analyze complex geometric shapes and different material models,

along with methods to replicate the porous nature of soils. The configuration of the RFS models can be seen in Figure 2.2, which consists of a semi-circular bulb on top of the main shaft with two roots extending through the bulb, at a 68.23° from the top surface of the bulb, and out to the positive and negative x-axis directions. There is also a 0.15 m (0.5 ft) extension extruding from the top of the bulb, which models the base of a signal pole and is used as a lever arm for the moment and lateral load to be applied. In Figure 2.1(b), the RFS configuration can be seen embedded within the soil.

A conventional foundation (control model) was made to compare all the RFS model's results. This model can be seen in Figure 2.1(a). The conventional foundation was modeled according to Idaho Transportation Department (ITD) standards for a 15.24 m (50 ft) tall traffic signal pole with a 15.24 m (50 ft) mast arm, which consists of a 0.91 m (3 ft) diameter circular foundation at a depth of 2.44 m (8 ft). In order to compare the proposed RFS with the conventional foundation, the lateral wind load and maximum moment experienced at the ground level of the foundation was determined. ITD specifies all signal poles must be designed to withstand 90 Mph winds. By using the 2001 AASHTO Wind Load Support Specifications (Fouad and Calvert 2003), the lateral wind load was calculated to be 2.35 kN (527.75 lb). Using Brom's method, the maximum moment experienced was back-calculated to be 115 kN-m (85.34 kip-ft). By applying the same lateral load and moment to both conventional foundations and RFSs, their performance can be compared.
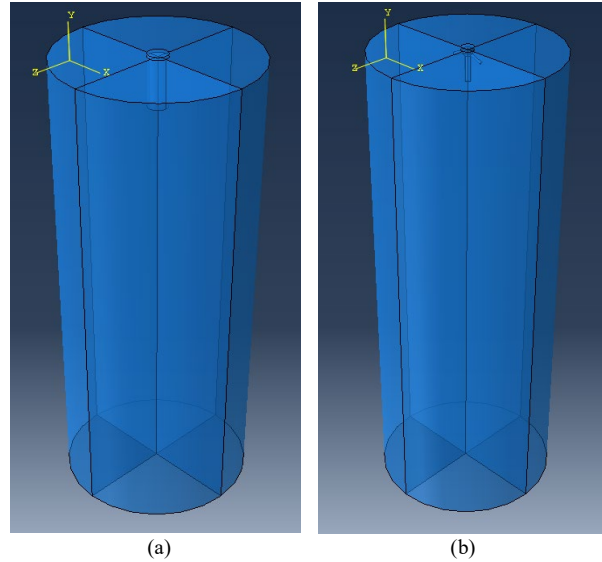
Figure 2.1. **(a) Conventional foundation embedded in soil (b) RFS system embedded in the soil**

When developing these models, three key variables were analyzed to find the optimum geometric configuration that could withstand the same moment and lateral load as conventional foundations while producing a relatively similar deflection. The three key variables were bulb diameter, root length, and shaft length. The selected variables to test were 0.46 m (1.5 ft) , 0.61 m (2ft) and 0.91 m (3 ft) and for bulb diameters; 0.46 m (1.5 ft), 0.61 m (2 ft) and 1.22 m (4 ft) for root lengths; and 0.91 m (3 ft), 1.23 m (4 ft) and 1.83 m (6 ft) for shaft lengths. A total of 27 models were made to investigate the effect of these three changing variables. The soil was modeled as a cylinder with a 9.14 m (30 ft) diameter and 24.38 m (80 ft) length to minimize any boundary effects.

Modeling Variables

For comparison purposes, the conventional and RFS material properties were modeled the same. The reinforced concrete foundation was modeled as an isotropic elastic material with a density of 2400 kg/m^3, young's modulus of 50 GPa, and a

Poisson's ratio of 0.3. The soil properties for the conventional foundation and RFS

models were kept the same as well. The medium dense sand was modeled as an

elastoplastic material and with a density of 1800 kg/m^3, young's modulus of 50 MPa, a

Poisson's ratio of 0.3, and a void ratio of 0.6. Mohr-Coulomb Plasticity model was used

to simulate the plastic nature of the soil. A detailed report of the input parameters for the

foundation and soil can be found in Table 2.1.1.

Table 2.1.1.   Model Input Parameters

Material	Parameters	*Value*	*Unit*
Foundation	Density	2400	kg/m^3
	Young's Modulus	50	GPa
	Poisson's Ratio	0.3	-
Soil	Density	1800	kg/m^3
	Young's Modulus	50	MPa
	Poisson's Ratio	0.3	-
	Permeability	0.00001	m/s
	Void Ratio	0.6	-
	Friction Angle	30	º
	Dilation Angle	10	º
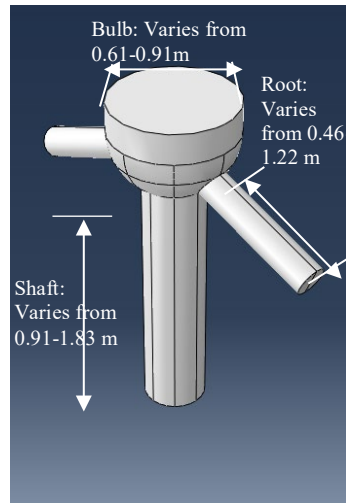
Figure 2.2. **RFS system showing the different variables studied in this research**

<u>Boundary Conditions and Loads</u>

The foundation was constrained in the assembly section by embedding the foundation in the soil. The sides of soil were constrained in the x and z-directions, the bottom of the soil was constrained in all directions, and the top of the soil was constrained with pore water pressure. This was done to model the effect of the sides and the bottom of the soil being constrained by the surrounding soil, allowing the top of the soil to deflect as it would in physical testing. Three steps were used to analyze the model; first, the initial step where all material properties are applied, followed by the geostatic step for the soil, and then a loading step. There was a -10 m/s^2 gravity load applied to the whole model. A 115 kN-m moment was applied in the z-direction to cause movement in the negative x-direction, and a 5 kN lateral concentrated force was applied in the negative x-direction. These forces were applied with a coupling of the center node and the surface of the 0.15 m lever arm that protrudes out of the soil.

Meshing and Element Types

The foundation and soil were meshed separately to analyze smaller sections of the

foundation and larger sections of the soil as well as limiting running time. The

foundations were given a 0.05 seed mesh and 10-noded quadratic tetrahedron (C3D10)

elements. C3D10 was selected due to its ability to mesh complex geometries uniformly

and consistently. The soil was given a 0.5 seed mesh and 8-noded trilinear displacement,

trilinear pore pressure, reduced integration, hourglass control (C3D8RP) element.

C3D8RP was selected to properly analyze the soil's pore fluid/stress. These seed values

were selected based on the preliminary trials and their results.

Results

Deformed Models

The resulting deformed shapes for both the RFS model and the control model,

magnified with a scaling factor of 500, are presented in Figure 2.3. From these visuals, it

is clear that in the RFS model, the deformation and impact of the loads are being

dispersed through the bulb and the right root, whereas in the control model, it is not being

dispersed. In the control model, much more of the deformation is concentrated on almost

half of the top and down the side of the foundation.

(a)

(b)
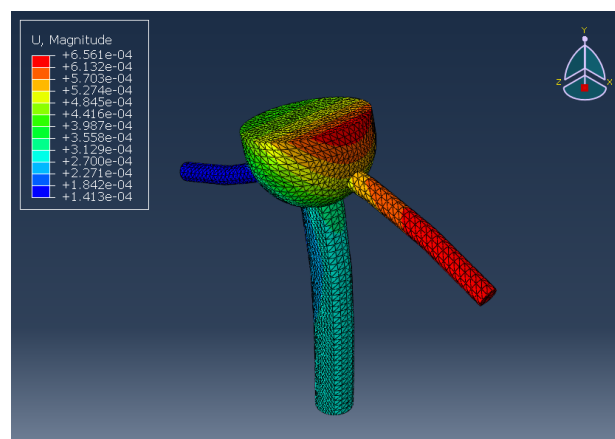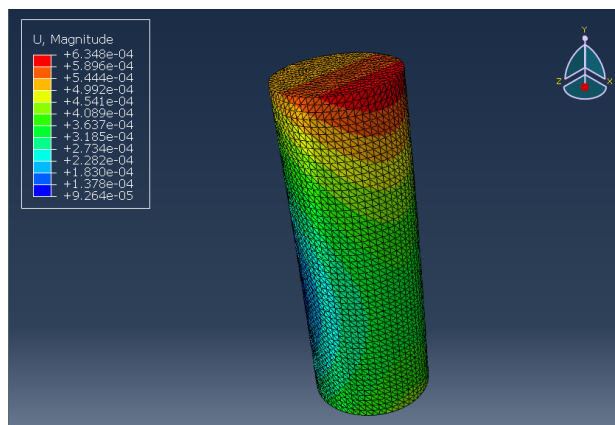
Figure 2.3.   (a) Deformed control model (m) (b) Deformed RFS (m)

The Effect of Shaft Length

All models were analyzed for stresses, strains, displacement, velocity, acceleration, forces, reactions, and contact. In this paper, the resulting displacement of the foundation systems was used to directly compare the conventional control foundation with the RFS systems. The control model produced a 0.552 mm maximum displacement. This displacement was then used to calculate the percent reduction of the resulting deflection of the 27 different RFS models compared to the control. However, it should be stated that according to (AASHTO 2016) for supports under Service I, experiencing dead load and wind load deflection should not exceed 10% of the structure's height. Therefore, some results do not reduce deflection compared to the conventional foundation but may have an acceptable deflection according to the standard.

The results have been categorized by their bulb diameters (as seen in Figure 2.4) to show the best configuration of root length and shaft length for each size of bulb diameter. It is apparent that different root lengths and shaft lengths yielded better deflections depending on their bulb diameter. Looking at the shaft lengths, specifically in Figure 2.4(a), for a 0.46 m bulb diameter, a reduction in deflection can be achieved with a root length of 1.22 m at shaft lengths of 0.91 m and 1.23 m. With a root length of 1.22 m, the -2% reduction could be acceptable. Whereas, at a shaft length of 1.83 m, a reduction in deflection cannot be achieved. In Figure 2.4(b), comparing shaft lengths at a bulb diameter of 0.61 m, only the 1.23 m shaft length experienced a reduction in deflection. In Figure 2.4(c), the results showed a reduction in deflection for all three shaft lengths with a root length of 1.22 m. It is evident that at a bulb diameter of 0.91 m, different shaft lengths can successfully be used.

For bulb diameters, 0.46 m and 0.61 m, a reduction of deflection was not achieved by 0.61 m or 0.46 m root lengths. Only with a 1.22 m root length could a reduction in deflection be achieved. However, it should be noted that for a 0.61 m bulb diameter, slight negative reduction occurred, which may possibly be an accepted deflection, even though it did not outperform the control model.
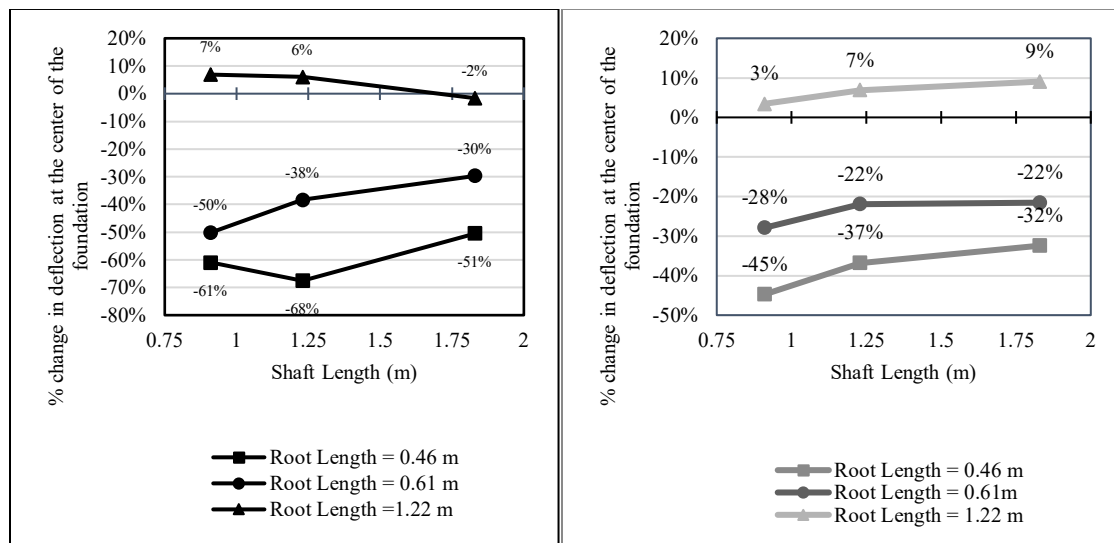
(a)

(b)
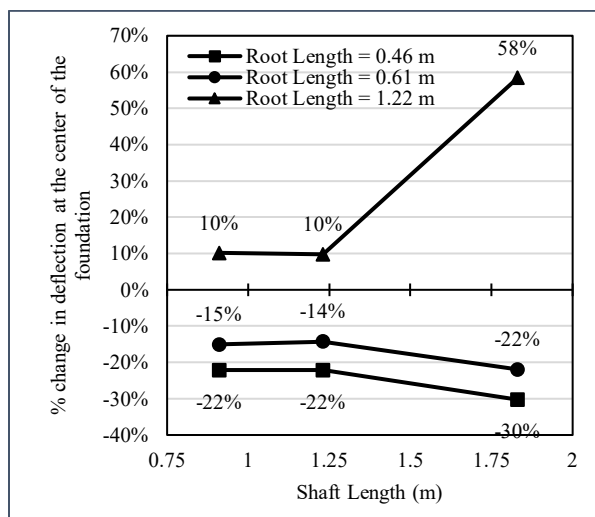
(c)

Figure 2.4.   Effect of shaft length (a) 0.46 m bulb diameter, (b) 0.61 m bulb diameter, (c) 0.91 m bulb diameter

The Effect of Root Length

In Figure 2.5, the effect of root length for the 0.91 m bulb diameter can be seen. This bulb diameter was chosen since it produced the highest reduction in deflection. The data showed that 0.91m and 1.23 m shaft lengths performed very similarly as the data lines are almost on top of each other. It is clear that a 1.22 m root length positive reduction is possible with varying shaft lengths, making this configuration the best combined with a 0.91 m bulb diameter.
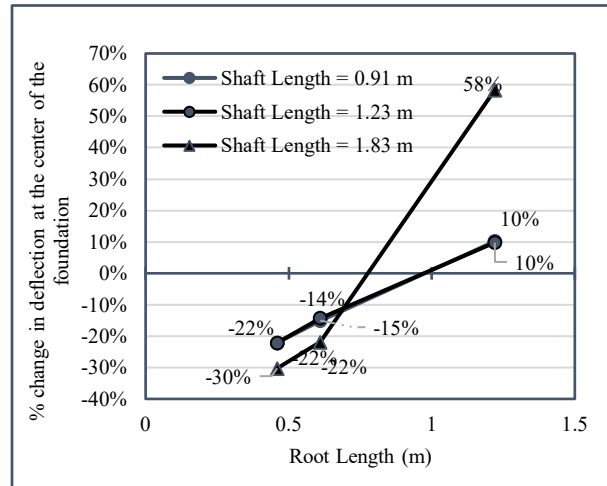
Figure 2.5.   Effect of root length for a 0.91 m bulb diameter

The Effect of Bulb Diameter

In Figure 2.6, a comparison between bulb diameters is made, concentrated on the 1.22 m roots since they performed the best. The 0.46 m bulb was fairly consistent and saw some reduction and minimal decrease in reduction. The 0.46 m bulb produced a reduction in deflection for shaft lengths other than 1.83 m, which saw a -2% reduction making it a configuration to avoid in the future as a possible RFS. All shaft lengths at a 0.91 m bulb reduced deflection, making this a bulb diameter that could have various shaft lengths and root length configurations that work well for various pole foundations.
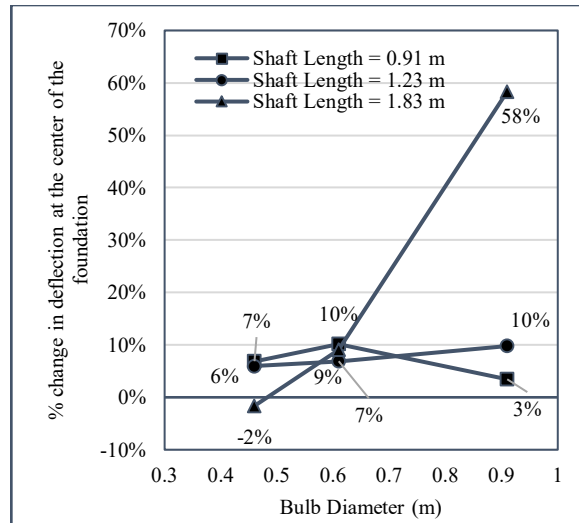
Figure 2.6. **Effect of bulb diameter, with 1.22 m roots at various shaft lengths**

Modeling Limitations

Although modeling software, like Abaqus, are a great way of testing a hypothesis in a time-efficient and analytic way, they also have limitations. This research topic is limited to being theoretical right now due to there being no physical testing yet accomplished. Therefore, these root models have not yet been calibrated with physical data. With physical test data, the model's properties, geometric configuration, constraints, and loads can be revised to better represent RFSs. Since this has not yet been done, these results, previously discussed, are theoretical but a good basis for further exploration with physical testing.

Summary

This study aims to investigate the feasibility of imitating biomimicry to create RFS systems. With the use of Abaqus, this new and innovative foundation system has been modeled and analyzed to conclude that an RFS system that is more environmentally friendly, economically efficient, and less invasive to the earth can be achieved. The main findings of this study are:

- An RFS consisting of a 0.91 m bulb diameter and 1.22 m root lengths are the optimum configurations. Specifically, combined with a 1.83 m shaft length produce a 58% reduction in deflection in comparison with a conventional foundation.

- It was found that a 0.46 m root length results in up to a -68% reduction in deflection, therefore making an unrealistic length for roots and should be ruled out. Similarly, a 0.61 m root length produced a smaller negative deflection reduction as well and should be analyzed further to investigate its feasibility of using it as a possible root length.

- It should also be noted that some models that produced a negative reduction in deflection that was minimal may still be a feasible configuration. They should not be ruled out just for not outperforming the conventional foundation.

Future work must be done to fully prove RFS systems are an alternative to conventional foundations. Although through numerical analysis, the best configurations for RFSs have been found, they still must be physically tested. Physical testing will include 3D printing the models that performed the best and testing them by placing them in a test apparatus that uses sensors to apply a load and record the resulting deflection. After physical testing is achieved, the models can be calibrated to better represent the performance of RFSs.

CHAPTER THREE: EVALUATING THE FEASIBILITY OF USING A TREE ROOT-BASED INNOVATIVE FOUNDATION ALTERNATIVE TO SUPPORT TRAFFIC SIGN STRUCTURES

Abstract

Trees create vast three-dimensional network of roots to support and anchor the critical above ground trunks, leaves, and limbs. In this work we investigate the feasibility of imitating such technique and create similar networks to support civil infrastructure, particularly those that are subjected to moment loads such as traffic signal posts. In this paper an attempt was made to evaluate the feasibility of a shallow tree root-based foundation system to replace the conventional deep foundations. Numerical simulations of various tree-root based foundation systems were conducted and compared with numerically simulated conventional foundation alternatives for a typical signal pole foundation used by the Idaho Transportation Department (ITD). The variables studied were the number of roots, root length and root depth. Results indicated that it is feasible to replace deep foundations using this novel foundation type and save costs and environmental impacts. In addition, it was noted that shallower root depths were more effective than deeper ones.

Introduction

Tall slender lightweight structures subjected to large overturning loads, such as sign structures, towers, or windmills, are commonly supported by conventional foundations such as mats, pile groups, and/or piled-rafts. These foundations are generally uneconomical

as they are typically overdesigned and as a result are expensive and have negative environmental impacts. It would be beneficial to develop an efficient foundation configuration that uses less materials and minimizes environmental and economic impacts. To develop such an efficient foundation system, one does not have to look further than tree roots. It is difficult to find a more efficient foundation system than the roots of a tree. Trees create vast networks of roots to support and anchor the critical above ground trunks, leaves, and limbs. Contrary to popular belief tree roots are very shallow in depth and are very close to the soil surface (< 2m), (Dobson 1995b). Among the different types of root architectures, *tap roots* seem to provide the strongest support due to the anchoring nature of this root system and are associated with trees such as white oak, hickory, walnut, etc…

Traffic sign structures are tall and slender like a tree. However, these structures are currently supported using deep foundations that are generally 2 ft to 3 ft in diameter and up to 10 ft in depth. By imitating tree roots, one should be able to develop an efficient foundation system that minimizes the need for deep foundations for slender structures. Hence, this research evaluated the feasibility of using a shallow root-based foundation system to support traffic sign structures. The following questions were raised: what would be the ideal depth of Root Foundation system? How far should the roots extend, both horizontally and vertically, to provide comparable support to a conventional deep foundation system? How many roots are needed to provide comparable support to a conventional deep foundation system? To answer these questions finite element models were developed for conventional, and tree-root based foundation systems and their lateral deflections under moment and lateral loads were compared. Variables such as length of the

secondary root, location of the secondary root as well as its inclination were studied. These results are presented in this paper.

Background

Biomimicry is the process of imitating (or getting inspired from) nature to solve various human problems (Benyus 1997b). The process involves emulation at three levels, form, process, and ecosystem (Benyus 2008). To fully learn from nature, a close examination of the three aspects is key. Trees have been engineering foundations from time immemorial. The ability of a tree root system to sustain tall above ground structure with a very shallow system of roots is quite fascinating. For example, red wood trees (Giant Sequoia), which grow over 300 ft in height only have root system that are shallow (six to eight feet) but extend about 100 feet from the trunk (National Park Service 2007). Adapting a similar method for urban civil engineering construction may not be feasible due to right-of-way issues, nevertheless, there are definitely lessons that could be learned by mimicking tree roots and using those lessons to develop efficient geotechnical foundation systems that do not use large amounts of raw materials and cause harm to the environment. Since the construction/building sector is one of the major contributors of Green House Gases (UN Climate Change News 2018; UN Environmental Program 2020), any improvements in methods and materials to minimize these impacts are highly welcomed.

A mature tree root system can be categorized into three broad groups: heart root, tap root, and plate root systems (Büsgen et al. 1929). As explained by (Stokes and Guitard 1997b), in a "heart" root system, both horizontal and vertical secondary roots develop from the base of the tree stem (see Figure 3.1). In the case of a "plate" root

system, horizontal roots spread from base of the stem with a tertiary sinker roots going vertical from the horizontal roots. The third type of root system has a large tap root anchoring the tree into the soil with secondary roots spread horizontally to act like guy ropes (Ennos 1993). In all these cases, the lateral roots or secondary roots are important in transferring the external loading forces into the ground. In this research, a tap root system was chosen due to their large anchoring system along with a lateral root system that can help resist moment loads from the signal posts.

Heart Root System

Plate/flat Root System
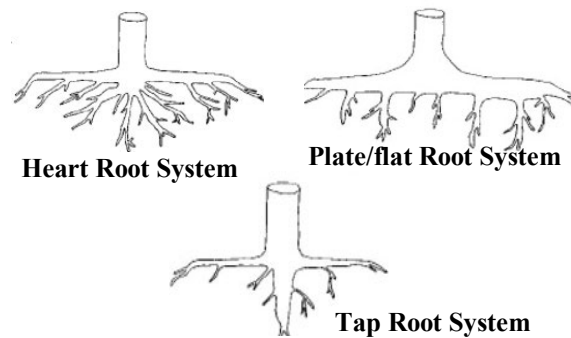
Tap Root System

Figure 3.1.   Three types of root systems (After (Rahardjo et al. 2009))

Rodriguez et al. (2020) conducted a state of practice (SOP) study that included twelve Departments of Transportation (DOTs) to document the foundation systems used by coastal departments of transportation to support coastal mast arm traffic signal structures. The SOP study revealed that the most commonly used foundation system was a single conventional drilled shaft. Occasional use of a drilled shaft with wing walls was reported, however, these were less common due to construction and installation difficulties. In coastal areas the drilled shaft diameters range from 2 to 5 ft with embedment depths ranging from 5 to 21 ft. Several failures of the signal mast structures were reported during the hurricanes and these failures are usually at the anchor bolts used to secure the mast to the foundation (Thiyyakkandi et al. 2016). In non-coastal areas these

diameters range from 2 to 4 ft with embedment depths up to 10 ft. The authors

hypothesize that similar supports can be obtained from much shallower depths by

designing the foundations inspired from tree roots.

Numerical Modeling

To test this hypothesis, numerical simulations of the conventional and tree-root

inspired foundation systems were conducted using the finite element modeling software

ABAQUS. The conventional foundation was modeled as per Idaho Transportation

Department (ITD) standards for a 15.24 m (50 ft) tall signal pole with a 15.24 m (50 ft)

mast arm, which consists of a 0.91 m (3 ft) diameter circular foundation at a depth of 2.44

(8 ft). To compare the proposed root foundation with the conventional foundation, the

lateral wind load and maximum moment experienced at the ground level were determined

as per ITD specs. ITD specifies all signal poles must be designed to withstand 90 Mph

winds. By using the 2001 AASHTO Wind Load Support Specifications, the lateral wind

load was calculated to be 2.35 kN (527.75 lb). The maximum moment capacity of the

above-mentioned foundation type was back-calculated using Brom's method for cohesive

soils, this was determined to be 115 kN-m (84.8 kip-ft). Torsional loads were not

included in this analysis.

Since a tap root-based root foundation was selected the variables evaluated were

the length of the secondary roots, location of the secondary root and the number of

secondary roots. The length and the diameter of the tap root were kept constant at 0.46 m,

diameter and 1.22 m embedment depth. Three variations of the secondary root length

were studied, 0.61 m, 1.22 m, and 1.83 m. Similarly, three variations of the secondary

root location were studied, top, middle and bottom. In addition, three variations of the number of secondary roots were studied 2, 4, and 8 roots.

Model Details

The control model consisted of a 9.1 m diameter, 24.4 m deep soil cylinder with a central shaft of 0.91 m diameter and 2.44 m depth. The soil section was determined to be ten times the diameter of the conventional drilled shaft foundation to avoid any boundary effects. Figure 3.2 presents an image of the simulated conventional foundation. Figure 3.3 shows a typical root foundation with 8 secondary roots of 1.22 m length at the top of the tap root.

Element Type and Mesh Size

The foundation and soil were meshed separately, to analyze smaller sections of the foundation and larger sections of the soil as well as limiting running time. After several trials the foundation part was assigned a 0.05 seed mesh and 10-noded quadratic tetrahedron (C3D10) elements. C3D10 was selected due to its ability to mesh complex geometries uniformly and consistently. The soil was given a 0.5 seed mesh and 8-noded, trilinear displacement, trilinear pore pressure, reduced integration, hour glasses control (C3D8RP) element. C3D8RP was selected to properly analyze the soil's pore fluid/stress.
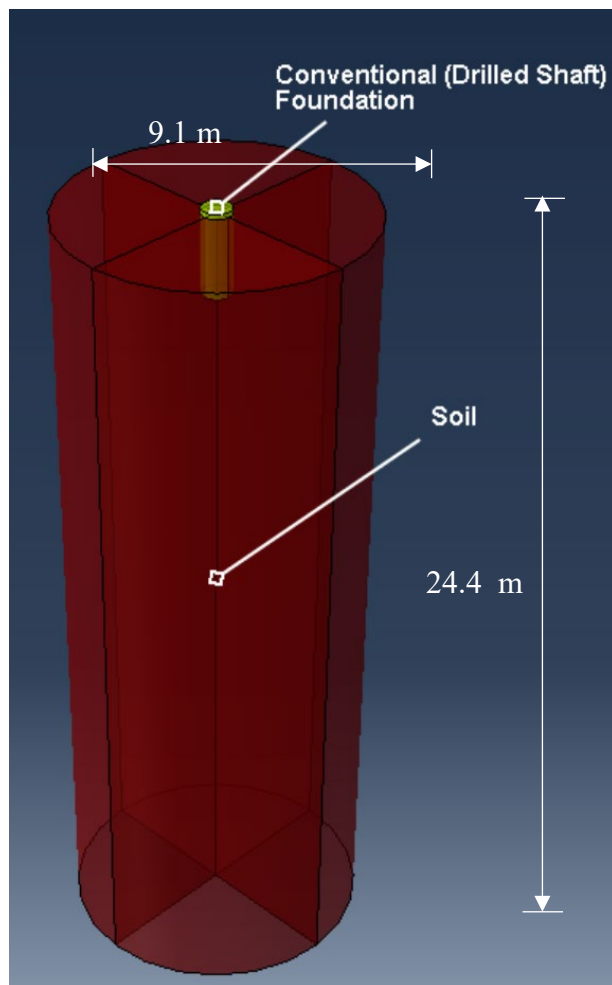
Figure 3.2. **FEM model of the conventional foundation system**
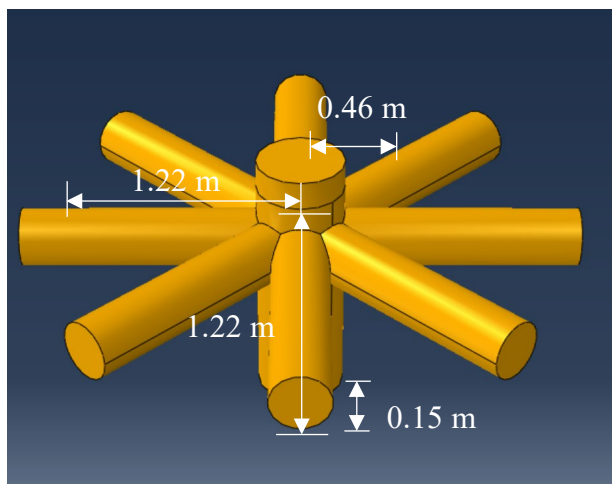
Figure 3.3. **Typical root foundation with eight secondary roots at the top of the tap root**

<u>Material Models and Properties</u>

For comparison purposes, the conventional and root foundation material properties were modeled the same. The foundation was modeled as an isotropic elastic material and had a density of 2400 kg/m^3, a young's modulus of 50 GPa and a Poisson's ratio of 0.3. The soil properties for the conventional foundation and root foundation models were kept the same as well. The soil was modeled as an elastic soil and was given a density of 1800 kg/m^3, a young's modulus of 50 MPa, a Poisson's ratio of 0.3, a void ratio of 0.6 and Mohr-Coulomb Plasticity. A detailed report of the input parameters for the foundation and soil can be found in Table 3.1.1.

Table 3.1.2.   Model Input Parameters

Material	Parameter	Value
Foundation	Density, kg/m^3	2400
	Young's Modulus, GPa	50
	Poisson's Ratio	0.3
Soil	Density, kg/m^3	1800
	Young's Modulus, MPa	50
	Poisson's Ratio	0.3
	Permeability, m/s	0.00001
	Void Ratio	0.6
	Friction Angle, deg.	30
	Dilation Angle, deg.	10

<u>Boundary Conditions and Steps</u>

The foundation was constrained in the assembly section, by embedding the foundation in the soil. The sides of soil were constrained in the x and z-directions, the bottom of the soil was constrained in all directions and the top of the soil was constrained with pore water pressure. This was done to model the effect of the sides and the bottom of the soil being constrained by surrounding soil, allowing the top of the soil to deflect as it would in physical testing. Three steps were used to analyze the model; first the initial step where all material properties are applied, followed by the geostatic step for the soil and then a loading step. There was a -10 N gravity load applied to the whole model as well as, an 115 kN-m moment applied in the z-direction and a 5 kN lateral concentrated force applied in the negative x-direction. The moment calculated according to Brom's method for conventional foundations was directly applied, however the lateral force calculated according to 2001 AASHTO was doubled and 5 kN was applied to test the foundations capabilities even further than what is required. These forces were applied with a coupling of the center node and the surface of the 0.5 ft (0.15 m) lever arm that protrudes out of the soil.

Results and Discussion

A total of 27 different root-foundation models were studied in this research in addition to the control model. Each root-foundation system (RFS) is denoted as follows n_1Rn_2L00X, where n_1 = number of secondary roots, R = root, n_2 = length of the secondary root, L = length, X = location of the secondary root, T = top, M = Middle, B = Bottom. Typical deformed mesh of the root-foundation model is shown in Figure 3.4. It can be noted here that the secondary roots in the direction of lateral load and moment (x-

axis) are experiencing deformation while the roots in the z-direction did not experience much deformation. The overall summary of results from the 27 models is presented in Figure 3.5. The dotted line in Figure 3.5 denotes the deflection (0.548 mm) obtained for the control section. It can be noted from the figure that 17 out of the 27 models had lower deflection than the control section indicating that these models have the potential to replace the conventional foundation systems for signal posts.
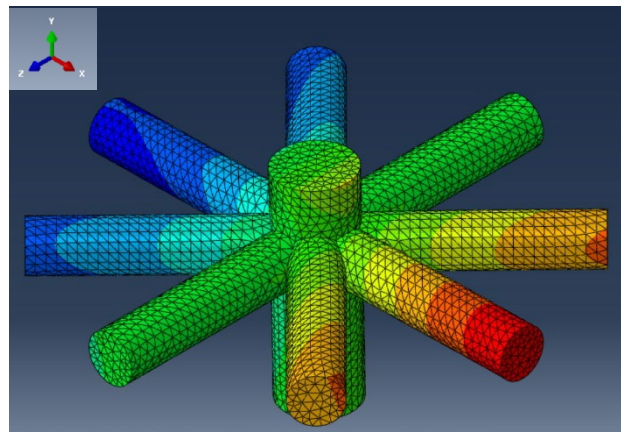

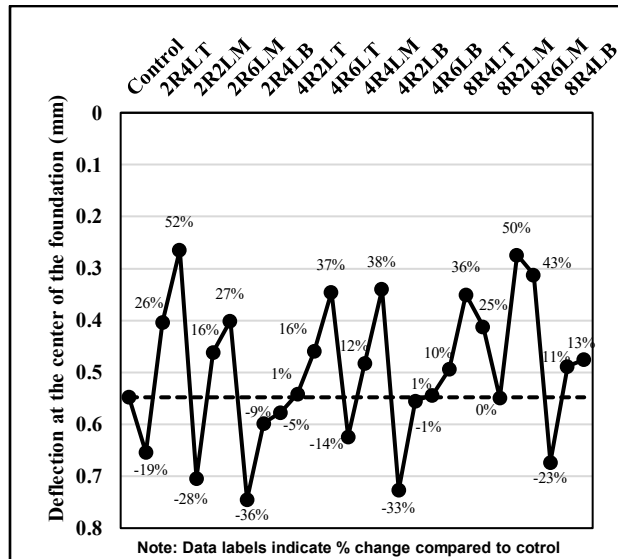**Figure 3.4.   Deformed mesh of the 8-root foundation model**

Figure 3.5.   Overall summary of deflection data obtained from the 27 models developed in this research along with the control

Effect of Root Length and Location

Figures 3.6, 3.7, and 3.8, present the variation of the percentage change in deflection for models with two roots, four roots and eight roots, respectively. For each of these graphs it is apparent that roots positioned at the bottom of the main shaft performed the least favorably. In Figure 3.6, a 1.83 m root length experienced the most notable reduction in deflection when placed at the top and middle of the main shaft. The 1.22 m root lengths experienced a reasonable reduction in deflection. Even when positioned at the bottom, a -1% reduction could be an acceptable performing foundation. The worst performing root length in Figure 3.6, is the 0.61 m root length which saw only negative deflection reduction. Making the two root, 0.61 m in length, a geometric configuration to avoid when designing a RFS. In Figure 3.7, four root RFS resulted in several viable geometric configurations. Similar to the two root RFS, the 1.83 m and 1.22 m root length performed the best when placed at the top and middle of the main shaft. The bottom positioning was only successful in reducing deflection if paired with the 1.83 m root length. Compared to the two roots RFS, the four root RFS can achieve a reduction in deflection with 0.61 m root lengths if positioned at the top. Four roots did lessen the negative reduction for 0.61 m root length's middle and bottom positioning by 7% and 3%, respectively. In Figure 3.8, eight root RFS outperformed two and four root selections for all root lengths. It is clear that for eight roots, middle positioning is the optimum choice. 1.22 m root length with middle positioning resulted in a 50% deflection reduction. 1.83 m root length experienced reduction in deflection for all positioning options. 0.61 m root length performed the best when designed with 8 roots, only experiencing a negative deflection when positioned at the bottom. Figures 3.6, 3.7 and

3.8 demonstrated the flexibility RFS have when designing a foundation, different root

lengths, positionings and number of roots can be selected for different foundation needs

while still out performing the conventional foundation.
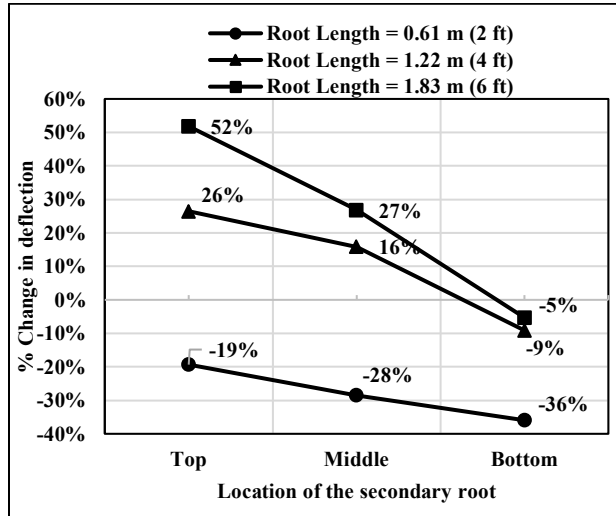
Figure 3.6.   Variation of % change in deflection with the location of the secondary root and its length for the root-foundations with two roots
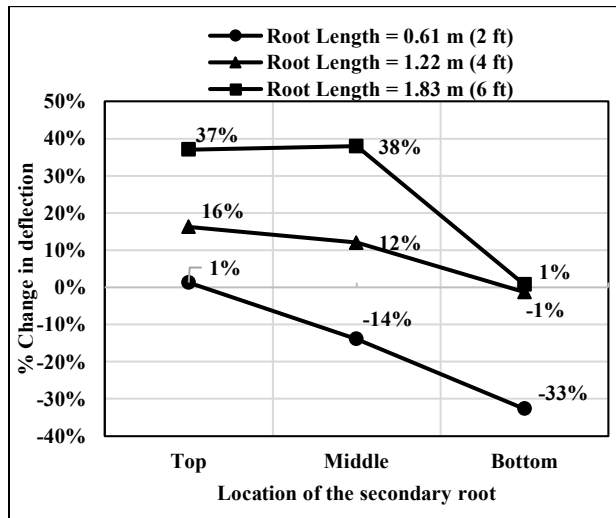
Figure 3.7.   Variation of % change in deflection with the location of the secondary root and its length for the root-foundations with four roots
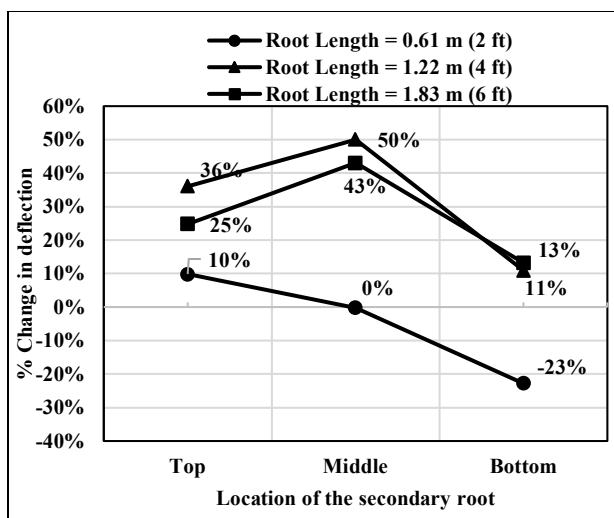
Figure 3.8. **Variation of % change in deflection with the location of the secondary root and its length for the root-foundations with eight roots**

Effect of Number of Roots

In Figure 3.9, the root length of 1.22 m results were compared to see the effect of two, four and eight roots and the location of roots. Straightway it can be seen that only the two roots, when positioned at the bottom, resulted in a negative deflection. The two roots positioned at the top, yielded the highest reduction in deflection of 52% and linearly declined with the positioning being lowered into the ground. The four-root system was consistent for top and middle placement resulting in a 37% and 38% reduction, respectively. The eight-root system was optimum when roots are placed in the middle resulting in a 43% reduction, but both top and bottom placement also saw a lower reduction. The argument can also be made that the 1.22 m root length provides the most consistent results, regardless of the positioning and number of roots it is paired with. Also, making 1.22 root lengths flexible in the foundation design process and has the potential to be designed specific to a structure's needs.

44

Figure 3.9. **Variation of % change in deflection with the number and location of the secondary roots for the root-foundations with root length of 1.22 m**

Summary

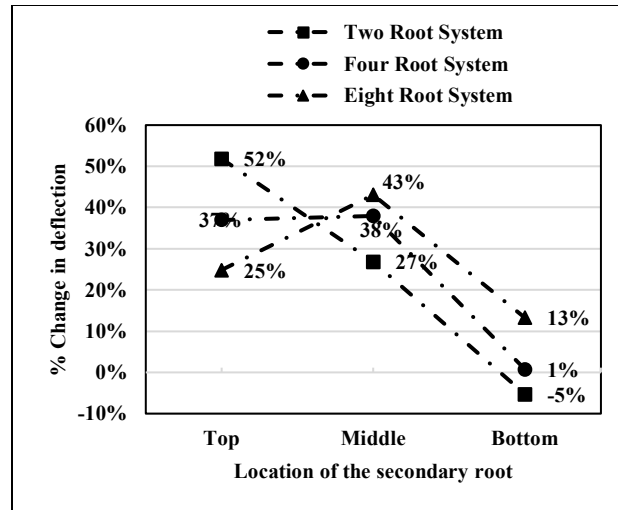Numerical modeling with the use of Abaqus has made it possible to test the newly proposed root foundation system and compare it to the performance of the conventional foundation. Not only has this study proved that analytically this new foundation is an option for tall, slender structures like traffic signal poles but it has also demonstrated the flexibility root foundation systems possess. The main findings of this study are:

- A RFS can achieve a lesser deflection than that of a conventional foundation. Specifically, when 1.22 m root lengths are used, they can be positioned at various depths to achieve a reduction in deflection. When roots are positioned at the top of the RFS the root lengths can be lessened to achieve reduction and cut back on material usage.

- Different RFS can be designed based on a structure's foundational requirements, to prevent overdesigning which can limit environment impacts, lessen our impact on the earth's surface and decreased foundational costs.

- 17 out of 27 models analyzed outperformed the conventional foundation.

Future work must be done to fully prove RFS are an alternative to conventional foundations. After all, the current work was primarily numerical modeling uncalibrated models. The research team plans to conduct physical testing on 3D printed best performing models. This test data will be used to calibrate the models and predict the results. These results will be published in future publications.

CHAPTER FOUR: EXPERIMENTAL AND NUMERICAL STUDIES TO EVALUATE THE FEASIBILITY OF TREE ROOT BASED FOUNDATION ALTERNATIVE

Abstract

Tree roots are an efficient foundation system trees create to sustain critical above-ground trunks, leaves, and limbs. This work takes inspiration from these naturally engineered systems to develop foundation systems to support civil infrastructure, particularly those subjected to high moments such as traffic signal posts. This foundation alternative is referred to as Root Foundation System (RFS). This paper studied the root system referred to as the taproot system. Both experimental and numerical studies have been performed to evaluate the feasibility of RFSs to support traffic signal poles. The best performing geometric configurations of an RFS were established through preliminary numerical modeling studies and these configurations were constructed from steel and physically tested in the laboratory. This physical testing data allowed the numerical models to be calibrated, and a parametric study was conducted. Results show that the RFS has excellent potential to replace the conventional deep foundation alternatives used to support traffic signal posts. They were able to provide similar or better support at shallower depths allowing cost savings from material reduction.

Keywords: Biomimicry, tree roots, innovative foundations, numerical modeling, finite element method.

Introduction

Tall, slender structures such as traffic signal poles are commonly supported by conventional foundations such as mats, pile groups, and pile-rafts which are typically expensive and have negative environmental impacts due to their use of large amounts of raw materials such as cement and steel. Many traffic signal poles have unnecessarily deep foundations, resulting in a variety of heavy metals and toxins being introduced to the soil we build on and ecosystems depend on (Setunge et al. 2009). With the large amounts of raw materials placed at these depths, harmful chemicals can seep into groundwater which can have a ripple effect on humans and the living organisms around us. A study completed by (Setunge et al., 2009) researched the environmental effects that freshly poured concrete into the soil had on a nearby waterway. This study showed how the freshly poured concrete resulted in water pollution, an increase in alkalinity, and the organisms that live in the water. Concrete can leach alkali into the water if placed nearby groundwater, a waterway, or another body of water. The high alkalinity in the water also caused fish to become distressed. Furthermore, this study noted that early-aged concrete could increase water pH levels to 11. It begs the question, how much damage to the soil, environment, and living organisms could we reduce by lessening the depth of such foundations and minimizing the amount of concrete used? With the growing concern for climate change, it is paramount that we decrease infrastructure's impact on the surrounding environment. Therefore, an attempt is made to develop a new and innovative type of foundation using biomimicry of tree roots, called the Root Foundation System (RFS). Tree root systems can be classified into taproot systems, heart root systems, and flat/plate root systems (Büsgen et al. 1929). In this research taproot system was used as a

source of inspiration as this type of system is easier to construct for civil engineering applications.

In this research, numerical simulations of various taproot-based foundation systems for traffic signal poles were conducted and compared with numerically simulated conventional foundation alternatives for a typical signal pole foundation. The variables studied were the number, length, and depth (location) of the secondary roots along the main root. Results indicated that it is feasible to replace conventional deep foundations using this novel foundation type and save costs and minimize environmental impacts. The results also showed that of all the taproots studied, three containing eight secondary roots close to the surface were the best performing. Hence, a scaled-down version of these three taproot systems was constructed using steel and physically tested in the laboratory. The laboratory tests were then used to develop a calibrated finite element model which was then used to scale up and predict the lateral load capacity of the full-scale taproot systems in comparison to the conventional deep foundation alternative. These results are presented in this paper.

Background

Biomimicry is the process of applying nature's tested strategies to solve complex human challenges (Benyus 1997a). It is not a new concept in today's world and has inspired many successful innovations. Several notable examples of biomimicry are bullet trains inspired by the shape of a king fisher's beak, helicopters inspired by dragonfly's wings, underwater signal transfer mechanisms inspired by dolphin communication, and the Eastgate Centre (shopping center) inspired by a termite mound to control the temperature naturally inside the building ("The Biomimicry Institute" 2020). Biomimicry

is a relatively new idea in the field of geotechnical engineering. Current research includes bio-inspired geotechnics inspired by organisms such as worms, ants, and termites to solve geotechnical problems such as soil excavation and penetration, soil exploration, soil-structure interaction, and mass and thermal transport in the soils (Martinez et al., 2021). This research expands biomimicry in geotechnical engineering to learn from one of the oldest living organisms, trees. For example, redwood trees which can grow up to 91.4 m in height with a 7.6 – 15.3 m diameter trunk weighing up to 500 tons and withstand 100 mph winds are supported by shallow root systems that radiate up to an acre laterally while only reaching 3.7 – 4.5 m in depth (Welker's Grove Nursery 2021). Although the sub-roots can grow to a depth of 4.6 m to 6.1 m, most remain within the top 0.30 m to 0.91 m of the topsoil. The reliability of redwood root systems in extreme weather winds makes them the perfect examples of foundation systems to learn from.

Tree root systems can be broadly classified into three groups: heart root, plate or flat root, and taproot systems (Büsgen et al. 1929). The heart root system has both horizontal and vertical secondary roots developed from the base of the tree stem (see Figure 4.1). In the case of a flat root system, horizontal roots spread from the base of the stem with tertiary sinker roots going vertical from the horizontal roots. The third type of root system has a large taproot anchoring the tree into the soil with secondary roots spread horizontally to act like guy ropes (Ennos 1993). In all these cases, the lateral roots or secondary roots are important in transferring the external loading forces into the ground. In this research, the taproot system was chosen due to its large anchoring system along with the lateral root system that can help resist moment loads from the signal posts. Typically, the taproot system can be found under the oak or pine trees.

Taproot System   Flat Root System   Heart Root System
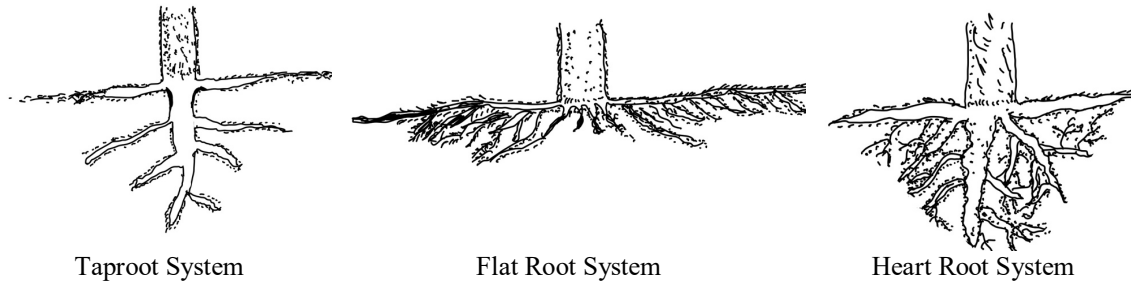
Figure 4.10   Three Common Tree Root Systems

Numerical Modeling Studies on Tree Root Systems

There have been previous works that have successfully modelled tree roots to solve engineering problems. In the study carried out by (Liang et al. 2017), they found that landslides caused by seismic conditions or large amounts of rainfall are typically improved or prevented by retaining walls, piles, or other similar traditional methods. However, they also found that the most efficient solution was also the most environmentally friendly, which is vegetation. Rather than planting vegetation and waiting months or years to see improvement, they decided to study root properties through geotechnical centrifuge modeling. The aim of their study was to provide a tree root model that can be tested multiple times in centrifuge modeling to portray a root system's spatial distribution, geometry, and mechanical properties more accurately. When studying the architecture of root systems, two types of influence zones were assigned: the critical root zone (CRZ) and the zone of rapid taper (ZRT). CRZ is approximately $\frac{1}{3}$ to $\frac{1}{2}$ the area that roots actually occupy and acts as a protection zone for the system. The ZRT has the dominant structural roots that make up 80% of the total root mass. The lateral roots that extend beyond the ZRT, span many meters and taper to

10-20 mm in diameter. Although, the lateral roots beyond the ZRT have lost much of their strength and rigidity. Regardless of the depth smaller roots reach, the majority of a root system's biomass lies in the topsoil and root density reduces as depth increases.

According to (Tobin et al. 2007), when shear loading is applied the peak strength of soil will be reached first followed by root enhanced shear strength until they fail. The models were 3D printed with an acrylonitrile butadiene styrene (ABS) plastic material and they were printed to a 1:10 scale to be suitable for testing. Four groups of root dimensions were defined as small, medium, large and coarse as well as two different types of root functions; root clusters and straight root groups. A total of 14 tests were completed on a large direct shear apparatus to test the elements that affect root and soil interaction and to support toe centrifuge test results. Their results showed that when shear loading was applied tap root systems were able to structurally transfer the loads through the system until they reached the smaller, deeper roots which often results in them breaking off from the cluster. They also found that the reinforcement of roots depends on confining stresses, depth of the slip plane given to roots and the root's morphology as well. When straight root groups were compared with clusters, the centrifuge results showed both types improved the slope stability problem compared to that of a conventional model. This study validates the use of biomimicry to solve engineering problems, finite element modeling's ability to accurately predict tree root behavior, and the benefits of using artificial tree roots.

Another study that advanced the capabilities of using artificial roots in engineering practice was aimed at simulating the effects of plant transpiration (Kamchoom et al. 2016b). Plant transpiration provides suction in soil which causes

increased soil strength and decreased water permeability, the artificial root system aims to provide these same properties. To achieve this the artificial root system was designed with a hydraulic head inside the root and can be lowered by vacuum being supplied and controlled. These artificial roots were made with a high air-entry value (AEV) filter, due to the small pore sizes this kind of filter provides. The water pressure the vacuum generates can be maintained in the water-saturated filter, so long as the vacuum is less than the filter. The result of upward water flow from the soil, through the filter can be achieved by the lower head being inside the root. A cellulose acetate (CA) was chosen as the porous filter due to its high AEV of 100 kPa and the hydraulic gradient can be maintained by any applied vacuum with this material. Furthermore, direct shear tests were conducted to investigate the soil-root interface friction under varying normal stresses. These tests showed CA has an elastic modulus of 83 MPa and a tensile strength of 31 MPa which is close to real tree root's properties. There were three tests carried out in soil boxes that allowed drainage; one test box has an artificial root system in it, one test box had a transplanted living tree in it and the last test box was the control in which nothing was placed in it. The soil used was a compacted, completely decomposed granite (CDG). The first stage of testing a -98 kPa constant vacuum was applied to the artificial root box for 48 hours while the living tree box was naturally producing soil suction. These boxes were also covered to prevent moisture loss through evaporation. Soil suction was measured by three tensiometers. The second stage of testing was a simulated 100 year rain fall period and the suction was again measured over time. The results showed the artificial root system and the tree achieved had the same suction. The same amount of vacuuming through the root depth was seen in the artificial root. Their results also

suggested the tree root and artificial root's ability to suction was deeper than the roots themselves. Overall, it was found that artificial root systems are capable of increasing soil strength and decreasing water permeability. Furthermore, this method could be applied to solve engineering problem such as stability slopes and evapotranspirative landfill covers.

Preliminary Numerical Analysis

As a first step in studying the effectiveness of RFSs compared to conventional deep foundation alternative, RFS inspired from taproot system and conventional foundation (cast-in-place pile foundation) were simulated using finite element modeling software ABAQUS. Different geometries of the RFSs were studied to establish the best performing RFSs to be tested in the laboratory. The conventional foundation was modeled as per Idaho Transportation Department (ITD) standards for light pole foundations (Idaho Transportation Department (ITD) 2017). As per this standard, for a 15.24 m (50 ft) tall signal pole with any mast arm length, the recommended foundation dimensions are 0.91 m (3 ft) in diameter and 2.44 m (8 ft) in length (embedment depth). This foundation was compared with several RFSs derived from the taproot system. A schematic of a typical taproot-inspired RFS is presented in Figure 4.2. The variables evaluated for the RFS were the length and location of the secondary roots. A total of 8 secondary roots were used at each location. The length and the diameter of the taproot were kept constant at 0.46 m, diameter, and 1.22 m embedment depth. Three variations of the secondary root length were studied, 0.61 m, 1.22 m, and 1.83 m. Similarly, three variations of the secondary root location were studied, top, middle and bottom. Each RFS is denoted as follows Z-n_lLX, where Z = RFS scale size; PFS = preliminary full scale, FS

= full scale calibrated, S = scaled, n_1 = original length of the secondary root (ft), L =

length, X = location of the secondary root; T = top, M = Middle, B = Bottom.
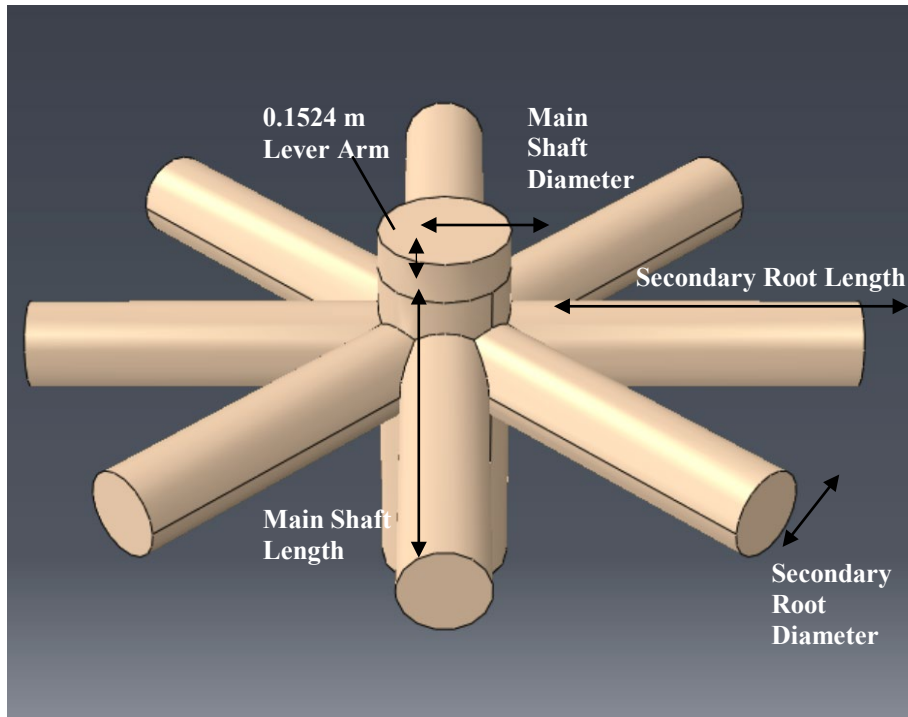
Figure 4.11   Schematic of a Typical Taproot-Inspired RFS

Model Details

The control model consisted of a 9.1 m diameter, 24.4 m deep soil cylinder with a

central shaft of 0.91 m diameter and 2.44 m depth. The soil section was determined to be

ten times the diameter of the conventional drilled shaft foundation to avoid any boundary

effects. Mesh convergence studies were performed to ensure that the foundation and soil

were optimized to save computational time without compromising the accuracy of the

model. The foundation part was assigned a 0.05 seed mesh and 10-noded quadratic

tetrahedron (C3D10) elements. C3D10 was selected due to its ability to mesh complex

geometries uniformly and consistently. The soil was given a 0.5 seed mesh and 8-noded

trilinear displacement, trilinear pore pressure, reduced integration, and hourglass control (C3D8RP) element.

For comparison purposes, the conventional and RFSs material properties were modeled the same. The foundation was modeled as an isotropic elastic material with a density of 7805.73 kg/m^3, a young's modulus of 200 GPa, and a Poisson's ratio of 0.25. The soil properties for the conventional foundation and root foundation models were kept the same as well. The soil was modeled as an elastic soil and was given a density of 1713 kg/m^3, a young's modulus of 7.58127 MPa, a Poisson's ratio of 0.3, a void ratio of 0.545, and Mohr-Coulomb Plasticity. A detailed report of the input parameters for the foundation and soil can be found in Table 4.1.1.

Table 4.3.1   Material Properties

Material	Parameter	Value
Foundation	Density, kg/m^3	7805.73
(Steel)	Young's Modulus, GPa	200
	Poisson's Ratio	0.25
	Poisson's Ratio	0.3
Soil	Density, kg/m^3	1713
(SC)	Young's Modulus, MPa	7.58127
	Poisson's Ratio	0.3
	Permeability, m/s	0.00001
	Void Ratio	0.545
	Friction Angle, deg	25.7
	Dilation Angle, deg	8.57

The sides of the soil were constrained in the x and z-directions, the bottom of the soil was constrained in all three directions and the top of the soil was constrained with pore water pressure boundary conditions to simulate saturated soil behavior. The foundation was loaded using a lateral force in the negative x-direction at a lever arm distance of 0.1524 m above the ground surface to all models studied. The lateral load capacity of a given foundation was estimated from the lateral load vs strain plot at a strain of 2.5%. The strain values in the model were calculated using the deformation in the direction of the applied force (x-direction) and dividing this value by the lever arm at

which the lateral load was applied. The maximum load capacity for traffic signal poles is restricted to a strain value of 2.5% according to AASHTO's Luminary and Traffic Signal Pole Standards (AASHTO 2016).

The lateral load vs strain plots for the nine RFSs and the control section are presented in Figure 4.3. It can be observed from this plot that the RFS that can withstand the highest lateral load is a system with 1.83 m root lengths. When 1.83 m root lengths are placed on the middle of the main shaft, they can withstand 240 kN of lateral force. The next best performing is the 1.22 m root length systems, with the top and middle locations performing similarly. It can also be observed that root lengths of 0.61 m, are capable of the lowest lateral load. It is also evident from this plot comparison, tap roots placed at the bottom decrease the RFS ability to resist lateral force.
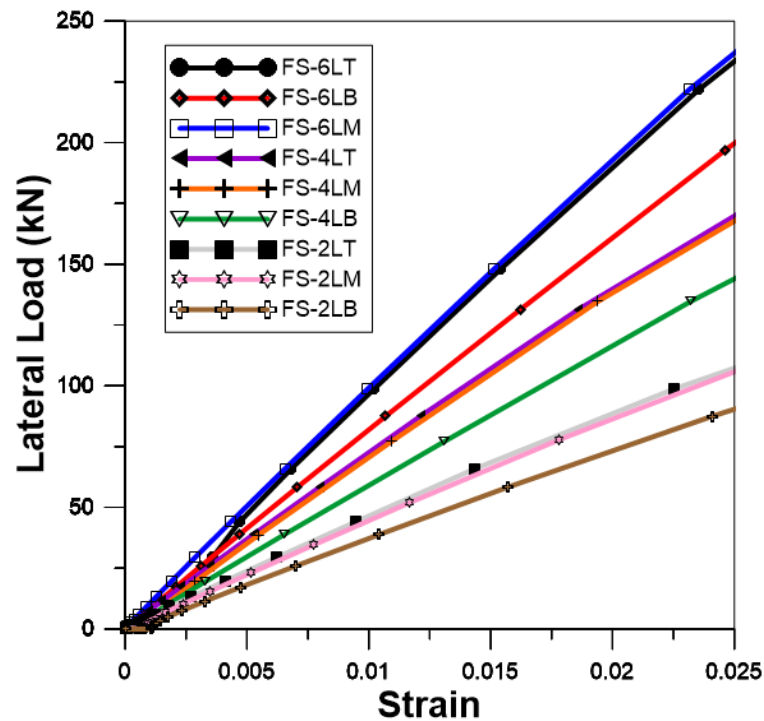
Figure 4.3   Lateral Load vs Strain Plots for the Nine Preliminary RFS Models Comparison
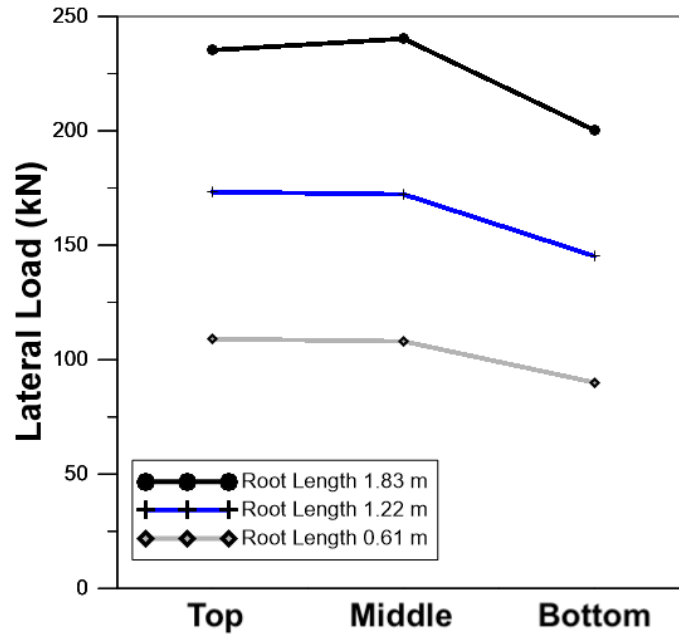
Figure 4.4   Preliminary Tap Root Models Lateral Load Comparison

Laboratory Testing

<u>Scaling Down the Model</u>

The preliminary models simulated RFSs at full size in a soil cylinder that was 9.14 m in diameter and 24.38 m in height, to avoid any boundary effects. As it was not feasible to physically test the RFS at full scale it was decided to test a scaled down version of the RFSs in the laboratory. Unfortunately, due to laboratory and financial constraints, the size of the soil cylinder could not be more than 0.305 m in diameter and 0.305 m in height which would represent the 9.14 m soil cylinder in the model. When the RFS were scaled according to the cylinder constraints, the resulting dimension of the secondary root was 0.00635 m, which introduces scale effects. Therefore, we decided to scale down using a ratio of 0.303 m (1ft):0.0127 m (0.5 in) to make them a reasonable size to test, with the expectation that boundary effects would be present. To negate the boundary effects both the RFS and control foundation were scaled using the same ratio.

The control foundation, which had a 0.91 m (3 ft) diameter and 2.44 m (8 ft) depth at full scale was scaled down to 0.038 m (1.5 in) diameter and 0.102 m (4 in) depth, respectively. In comparison, the scaled down RFS had a taproot (main root) diameter of 0.019 m while the secondary root had a diameter and length of 0.006 m and 0.076 m, respectively. The scaled models were made from low carbon steel rods that were welded together to form the required tap root specifications, as seen in Figure 4.5. Table 4.2.1 displays the various scaled dimensions of two RFSs physically tested. There is also a 0.15 m root stem extending off the top of the RFS and control foundations which acts as a lever arm for the force to be applied. This lever arm is also used to calculate the lateral strain according to AASHTO's Luminary and Traffic Signal Pole Standards, (AASHTO 2016). Each RFS is denoted as follows $Z\text{-}n_1LX$, where Z = RFS scale size; PFS = preliminary full scale, FS = full scale calibrated, S = scaled, n_1 = original length of the secondary root (ft), L = length, X = location of the secondary root; T = top, M = Middle, B = Bottom.
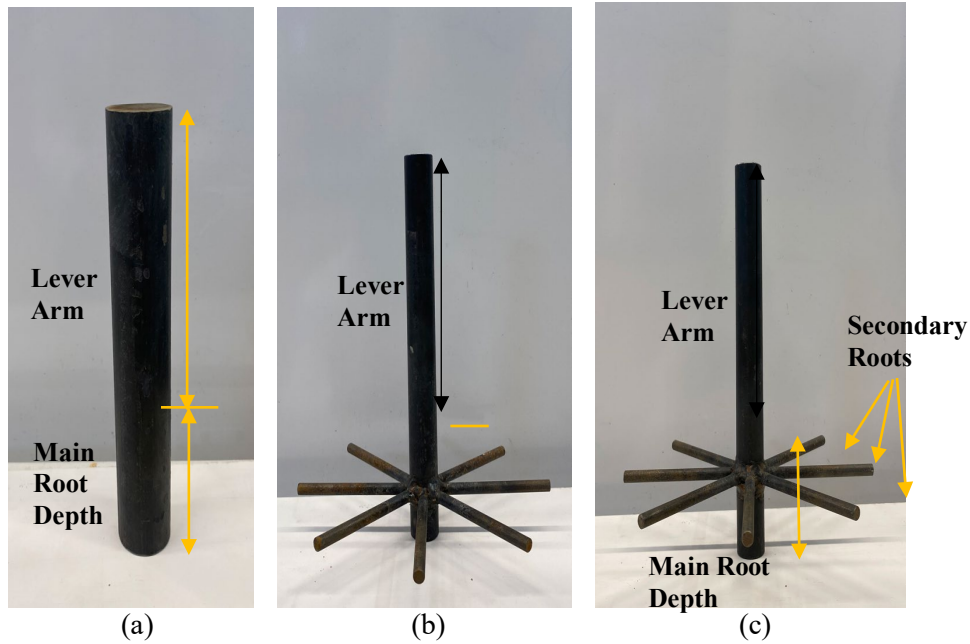
Figure 4.5 **Physically Tested Foundation Systems (a) Control (b) S-6LM (c) S-6LT**

Table 4.2.4. **Steel Root Dimensions**

	S-6LT	S-6LM
Main Root Shaft Depth (m)	0.051	0.051
Main Root Shaft Diameter (m)	0.019	0.019
Secondary Root Diameter (m)	0.006	0.006
Secondary Root Length (m)	0.076	0.076
Location of Secondary Roots on Main Root Shaft	Top	Middle
Number of Secondary Roots	8	8
Angle Between Main Root Shaft and Secondary Root	90°	90°

Soil Properties and Experimental Setup

An artificially mixed soil was used to test RFS and control foundation. The soil contained 75% of a locally sourced medium dense sand and 25% of a locally-sourced cohesive soil. Various laboratory tests were conducted on the artificial soil mixture to obtain the soil properties presented in Table 4.3.1. The ASTM standards these laboratory tests were conducted according to can also be found in Table 4.3.1. The physical tests were completed in a 0.305 m diameter by 0.305 m height soil cylinder. The soil was compacted to its optimum moisture content and maximum dry density. However, it should be noted that the top 0.102 m of soil, where the foundations were placed, was harder to ensure uniformity of compaction than the bottom 0.203 m of soil since it had to be done around the foundation area and more care was taken not to damage the RFS. The control foundation's compaction was much easier to ensure compaction was uniform due to no lateral roots being attached to it. Therefore, it can be concluded that the control foundation's compaction was accurate.

The physical testing apparatus was constructed with two purposes in mind; applying a lateral load to the root stem lever arm and recording the deflection as load is applied. Figure 4.6 provides a schematic and physical picture of the testing system. As seen in Figure 4.6, the soil cylinder was placed in the testing frame and movement of the soil cylinder itself was restricted by a ratchet strap. This allowed only the displacement of the root within the soil to be measured. The root stem was then aligned with the force cell so the plate sensor could measure the force exerted on the RFS. A linear actuator, programmed to apply load at 1 mm/min, then applied a lateral load through the force cell. The displacement was determined by measuring the amount of movement the force cell

would move. All force and displacement data were collected via a data acquisition

system.

(a)   (b)
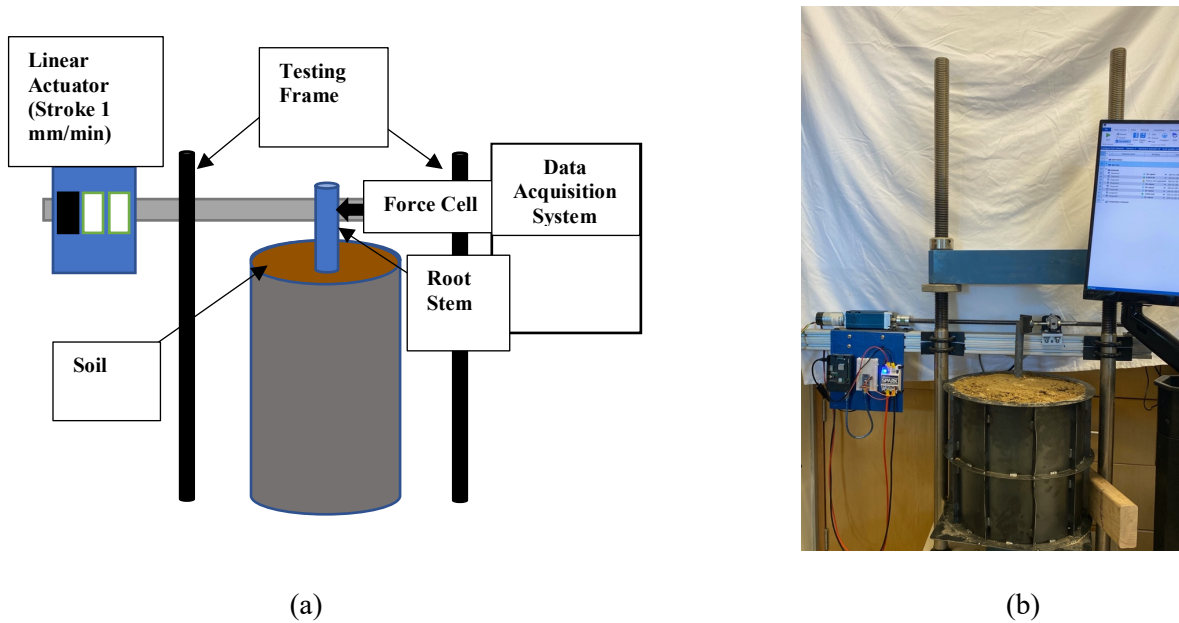
Figure 4.6   (a) Physical Testing Schematic (b) Physical Testing Apparatus

**Table 4.3.5.   Geotechnical Properties of the Artificial Soil Used in this Research**

Soil Property	Value	ASTM Testing Standard
Maximum Dry Density (kg/m^3)	1713	D-698
Moisture Content (%)	16.8	D-698
Specific Gravity	2.65	D-854
Elasticity (MPa)	7.58127	D-3080
Permeability, k (m/s)	1.0 E-5	D-2434
Void Ratio	0.54	N/A
Poisson's Ratio	0.30	N/A

Results and Discussion

The force and strain from the scaled physically tested RFSs and control can be found in Figure 4.7. The strain was calculated according to (AASHTO 2016), which states traffic signal poles strain shall not exceed 2.5% strain of the structure's height. Therefore, each physically tested model's displacement results were divided by the 0.1524 m (6 in) lever arm, which acted as the height of the structure, where the lateral force was applied. It is upon this basis that Figure 4.7's results are restricted to 2.5% strain.

These physical laboratory results highlight how difficult it was to compact the RFS models. The two tap roots only had one difference among them, the location they were placed on the main shaft. Therefore, it would be reasonable to expect their capacity curves to at least behave similarly. Instead, they have very different load patterns which indicates the uniformity of compaction was different for each RFS. Another take away from this data is a scaling limitation. It is difficult to replicate the resistance of a RFS's secondary root in the laboratory. It is also difficult to ensure the compaction directly under each lateral tap root is achieved. Since the control's compaction can be ensured, this data is deemed acceptable and will be the basis for calibrating the scaled control and RFS numerical models.
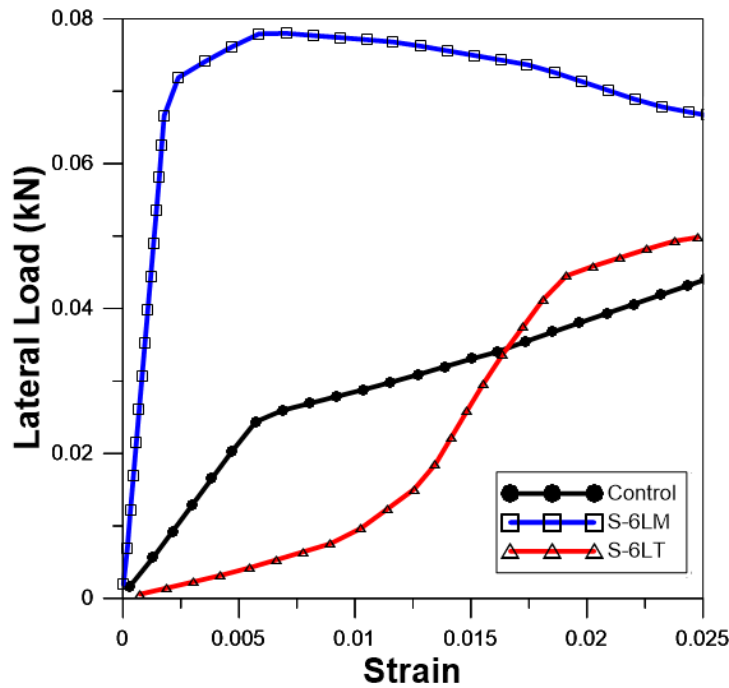
Figure 4.7   Physically Tested Lateral Load Capacity Results

Numerical Modeling

<u>Model Description</u>

Finite element modeling of the laboratory tested control foundation was conducted using Abaqus. The procedure was similar to the preliminary numerical modeling with minor changes to material model, full description of the modeling details are provided here for the sake of completeness. The control foundation was modeled to the exact dimensions they were made at, as seen in Figure 4.4. Similarly, the soil was modeled as a 0.305 m diameter and 0.305 m height soil cylinder with the same properties determined in the laboratory and are provided in Table 4.3.1. A direct shear test was also performed on the soil to obtain the elasticity and the cohesion yield stresses of the soil. The foundations and soil were made as separate parts and combined through the embedded region constraint. Three steps were used in these models; an initial step to load

all data, a geostatic step for the soil, and a soil load step which applied the lateral force and transient consolidation. The lateral load was applied to the same side and top of the 0.15 m lever arm, just as it had been done in the physical tests. A 0.01 mesh seed size was applied to both parts. The foundation was given 4-noded, linear tetrahedron (C3D4) elements and the soil was given 8-noded, trilinear displacement trilinear pore pressure with reduced integration (C3D8RP) elements. Boundary conditions were given to the sides of the soil cylinder which resisted movement in the x and z directions, the bottom of the soil cylinder resisted movement in all three directions, and the top of the soil was given a pore pressure boundary condition. Figure 4.8 provides an image of what these models look like when they have completed their simulations. Figure 4.8 (a) shows the displacement contour results of the entire model while Figure 4.8 (b) shows the displacement contour results of the control with the soil removed, to provide a look at the foundations movement under the soil.

(a)   (b)
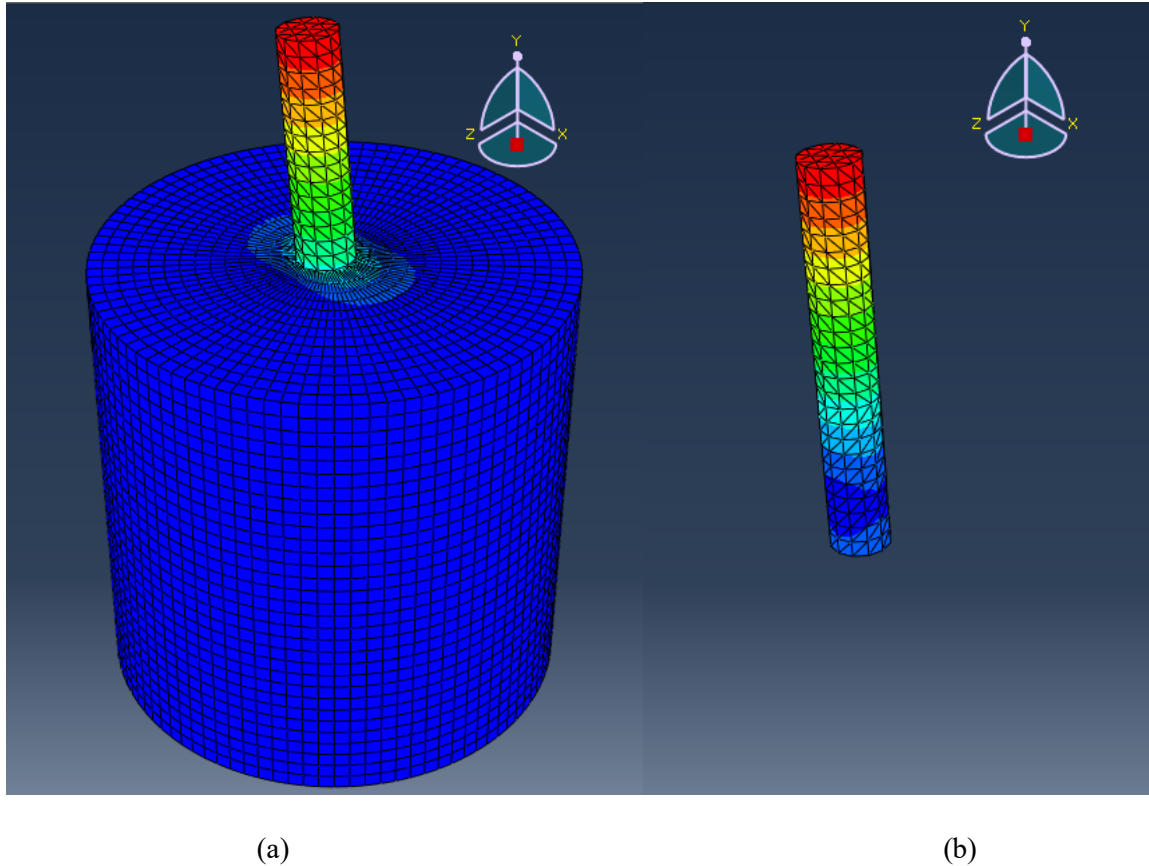
Figure 4.8   **(a) Scaled Control Foundation Embedded in Soil (b) Scaled Control Foundation**

Model Calibration

Since the physical control's compaction was done uniformly, in the laboratory, these physical results were used to calibrate the scaled down numerical model. First, the soil was calibrated by inputting the soil's direct shear results to get an accurate model of the soil behavior. These stress and strain values were inputted into the models to calibrate the soil to the physical properties. Abaqus used these values to graph and find the ultimate and yield stresses. Then the maximum force the physical model experienced in the laboratory was applied to the model's 0.15 m (6-inch) lever arm. Using the (AASHTO 2016), traffic signal pole standard the control model's strain values were found by dividing the control model's displacement by the 0.15 m (6-inch) lever arm

height. Figure 4.9 compares the control's physical and numerical modeling results up to
an allowable strain of 2.5%. Based on these results, it is clear the control's numerical
model is calibrated to the physical results. To further prove the control is calibrated with
the physical data, a statistical polynomial regression fit was ran to directly compare the
predicted and experimental data. Figure 4.10 shows the correlation between the control's
model strain results on the x axis and the control's physical strain results on the y axis.
The data points correlate very closely with a linear regression fit line. The coefficient of
determination, R-squared, between the physical and model results is 0.9998. Therefore,
the control model is deemed acceptable and calibrated.
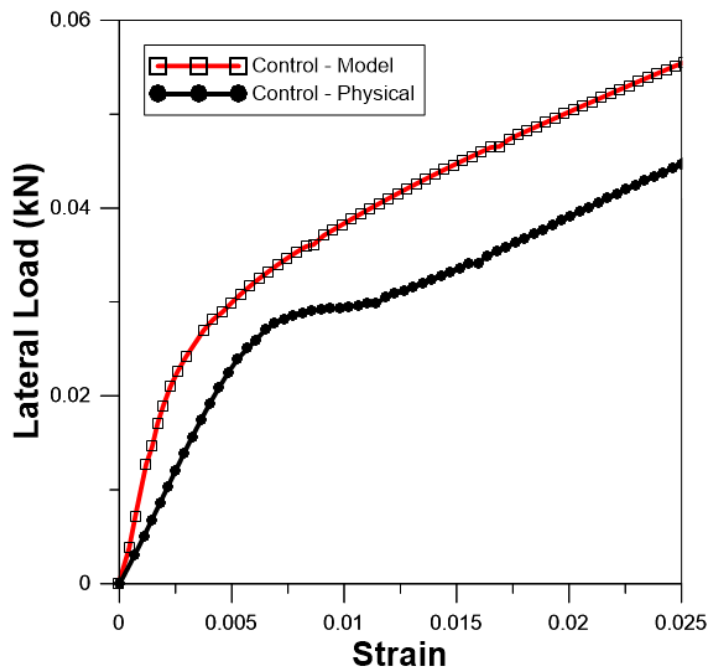
Figure 4.9   Control Physical and Model Lateral Load Capacity Comparison
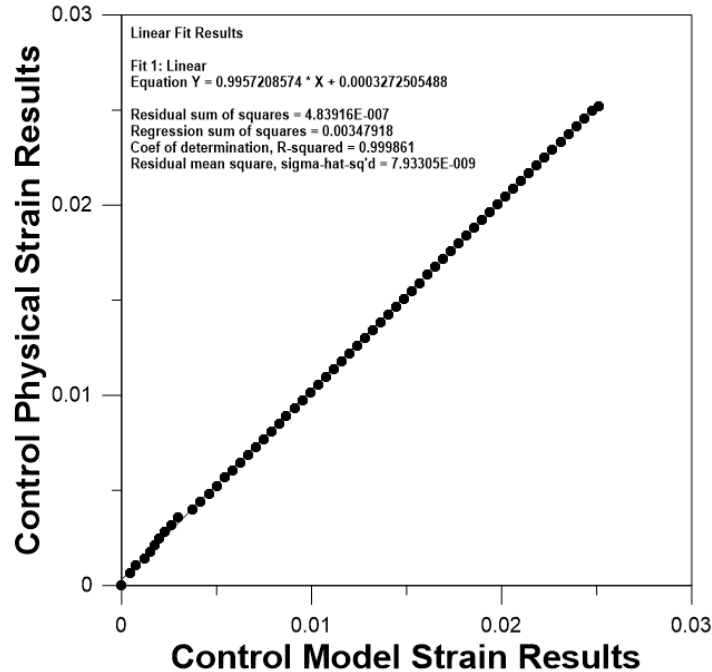
Figure 4.10   Control Physical and Model Strain Polynomial Regression Fit

Modeling RFS Using Calibrated Model

Since the physically tested RFS models' compaction could not be ensured, the

best way to compare the RFS's actual performance is by numerically modeling them

using the calibrated control model. The final scaled RFS were modeled according to the

control's calibrated numerical model. By applying the same constraints, properties, and

calibration methods to the RFS models, all numerical models can be compared. While it

was difficult to imitate the resistance an RFS would have in the laboratory, the numerical

models do not have that problem when calibrated as the compaction is uniform.

Once the RFS models had been calibrated to the control model, a lateral load was

applied until a 2.5% strain was achieved. This allowed the capacity of each scaled RFS to

be found. Figure 4.11 compares all the calibrated numerical models. The S-6LM RFS

performed the best as it was able to achieve roughly 0.18 kN while maintaining an

acceptable strain. The S-6LT RFS performed similarly but the capacity is slightly lower,

at roughly 0.16 kN. The control had the lowest capacity at 0.05 kN. These results indicate that all the RFS configurations have a higher capacity than the control foundation.
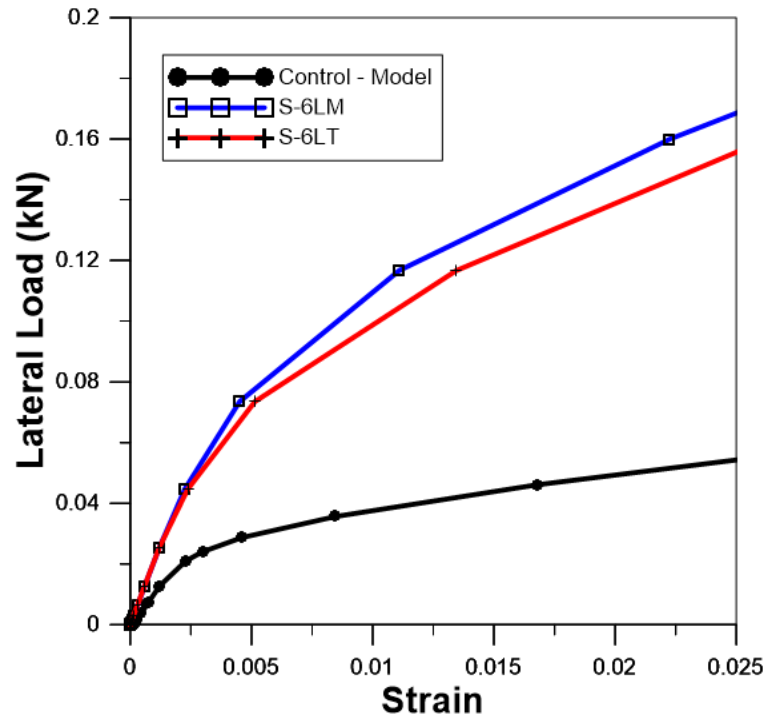
Figure 4.11   Numerical Model Lateral Load Capacity Results

Full Scale Numerical Models

The above comparisons demonstrate that the tested scaled down RFSs have better capacities than the control foundations. However, to fully understand the capacities of RFS, full scale models previously completed in the preliminary analysis were calibrated with the scaled data, properties, and constraints to compare their results. The control foundation, which is the conventional foundation in practice, was modeled with its standard 0.91 m diameter and 2.44 m depth. After applying all calibration methods, its capacity was compared with all four full scale RFS modeled capacities. Table 4.4.1

defines all four full scale RFS models' dimensions. Figure 4.12 provides a lateral load

capacity comparison that shows the control has a 42 kN capacity within the ASTM strain

standard. The FS-6LT and FS-6LM performed very similar and had a 180 kN and 185 kN

lateral load capacity, respectively. The FS-6LB resulted in a 165 kN capacity.

These results indicate that RFS can outperform conventional foundations by

roughly three times their capacity. Various models were then made to find the smallest

possible RFS that roughly the same 45 kN lateral load capacity as a conventional

foundation. The smallest RFS possible has a similar structure as the FS-6LM, but the

main shaft depth and tap root length has been decreased. Table 4.4.1 also provides a look

into how much material could be reduced if RFSs were used instead of conventional

foundations. This was calculated by finding the volume a conventional foundation and

RFS have, then find the percent reduction. The smallest possible RFS that has a similar

capacity as a conventional foundation, could save 87.71% of the material placed into the

ground. This reduction could save time excavating, the cost of a foundation, and reduce

the environmental effects a foundation has. With the depth of the smallest possible RFS

being only 0.91 m, this reduces the chances of raw materials effecting groundwater,

living organisms, and world around us.

Table 4.4.6.   Full Scale Steel Root Dimensions

	FS-6LT	FS-6LM	FS-6LB	FS-1LM
Main Root Shaft Depth (m)	1.22	1.22	1.22	0.91
Main Root Shaft Diameter (m)	0.46	0.46	0.46	0.46
Secondary Root Diameter (m)	0.15	0.15	0.15	0.15
Secondary Root Length (m)	1.83	1.83	1.83	0.31
Location of Secondary Roots on Main Root Shaft	Top	Middle	Bottom	Middle
Number of Secondary Roots	8	8	8	8
Angle Between Main Root Shaft and Secondary Roots	90°	90°	90°	90°
% Material Volume Reduction	70.92%	70.92%	70.92%	87.71%
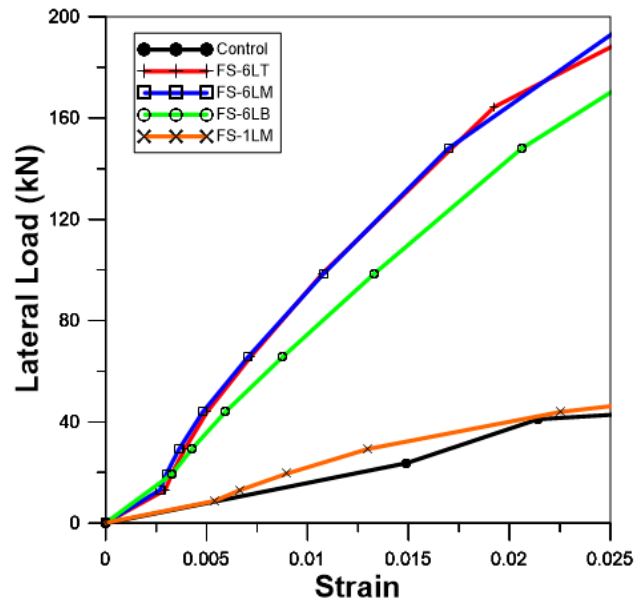
Figure 4.12   Full Scale Numerical Model Lateral Load Comparison
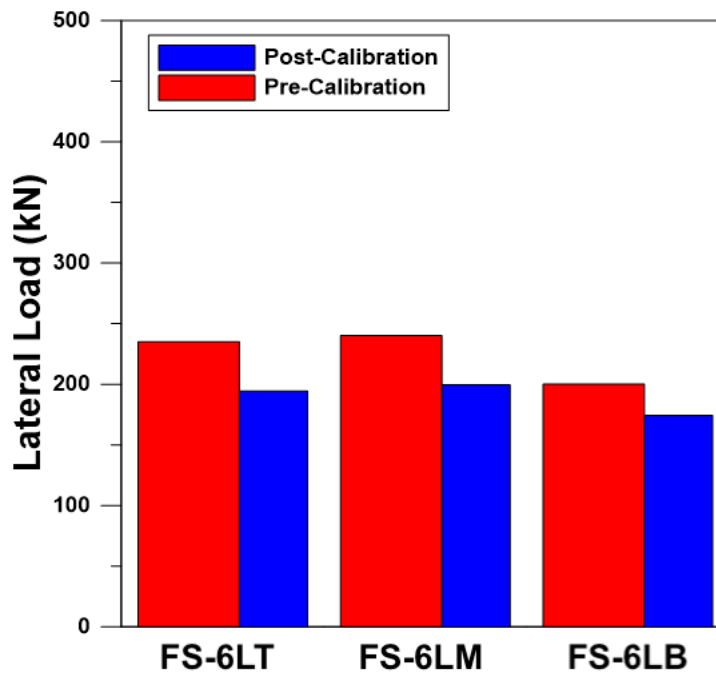
Figure 4.13   Full Scale Preliminary Numerical Models Compared to Full Scale Calibrated Numerical Models

Figure 4.13 provides a comparison between the full scale preliminary and calibrated models. The red bars corresponds with the preliminary full scale lateral load capacity and the blue bars correspond with the full scale calibrated lateral load capacity. Both FS-6LT and FS-6LM resulted in a 235 kN and 240 kN capacity, respectively, prior to calibration. After calibration FS-6LT and FS-6LM resulted in a 195 kN and 200 kN capacity, respectively. Both FS-6LT and FS-6LM indicate a 40 kN reduction of capacity once calibrated. Similarly, the FS-6LB had a 200 kN capacity prior to calibration and a 175 kN capacity after calibration was applied. The FS-6LB experienced a 25 kN reduction after calibration. Figure 4.13, highlights the importance of calibrating the numerical models to the soil's stress and strain values. This is a vital step in the RFS numerical modeling and provides Abaqus with an accurate description of the soil so it can provide an accurate response from the soil.

Study Limitations and Future Work Recommendations

Although this work provides a strong basis for RFS, future work must be done to prove RFS is an effective foundation alternative in the field. The scaled physical testing that was conducted during this study was limited in its ability to provide uniform compaction and simulate the resistance a RFS's secondary root would have under 1.22 m of soil when only 0.051 m cover the roots. Future work should include physical testing on a full scale, or at least on a scale at which compaction and boundary effects will not occur. Full scale physical testing will also allow different variations of compaction methods to be tested, to find the best way to ensure a uniform compaction is done. Physical testing at a full-scale will allow multiple possible RFS materials to be tested. For example, trying pre-cast concrete to form RFS geometries, liquid steel shape casting, and welded steel. Future work must also develop a complete construction method so it can be performed by others.

Future work must also include numerical model development. Numerical models should simulate various soil types, as this study focused on a medium dense sand. It should be noted that this would require stress/strain tests to be conducted on various soil types to accurately calibrate the models. Another area of interest is modeling real tree root systems more precisely as they grow in the soil. More numerical models ran with various soil types, root geometries and RFS material types will improve the confidence of these models being predictive. The ultimate goal of these numerical models is to develop one model that can be used to provide the best RFS for the engineering problem at hand.

Summary and Conclusions

This study aims to investigate the feasibility of imitating biomimicry to create RFSs. Preliminary numerical modeling identified the best geometric configurations of RFSs to physically test. Two scaled RFSs and a scaled conventional foundation were physically tested to find the force they could withstand and the displacement that occurred. The main findings of this study are:

- While physically testing the RFSs, it was difficult to ensure compaction was uniform due to the small scale the testing was done at. However, the physically tested scaled control's compaction was ensured and those results made it possible to calibrate accurate numerical models.

- The calibrated numerical models' results support the hypothesis that RFS have a higher capacity than the current conventional foundation in practice.

- Full scaled models demonstrated the smallest possible RFS that can perform similarly to a conventional foundation's capacity. All RFSs can reduce the amount of material used, the depth at which the foundation is place, and the environmental impacts foundations impose on the world around us.

RFSs are a more environmentally friendly and economically efficient method while being less invasive to the earth.

CHAPTER FIVE: SUMMARY AND FINDINGS

Summary

This research investigated the feasibility of root foundation systems (RFS) as an alternative to conventional foundations. This study was completed in three stages. First, preliminary modeling was conducted with the finite element method software Abaqus to identify the best performing RFS geometric configurations, out of 54 models. Second, the three best performing RFSs were scaled down and physically tested by applying a lateral load to the lever arm and collecting the resulting displacement. Third, using the physical testing results to calibrate the numerical models to make them accurate.

Major findings from this study are provided below:

1. Calibrated full scale RFS models demonstrate a lateral load capacity four times that of a conventional foundation. The smallest possible RFS that has a similar lateral load capacity as a conventional foundation, can reduce the foundation material by 87.71%.

2. Comparisons between preliminary full-scale models and calibrated full scale models, highlight the importance of applying a given soil's stress/strain data to calibrate numerical models.

3. RFSs are a more environmentally friendly and economically efficient method while being less invasive to the earth.

Recommendations

This study confirms that RFS have a place in geotechnical engineering and foundation alternatives. However, future work must be done to prove RFS is an effective foundation alternative in the field. Some recommendations for future work are provided below:

1. Full scale physical testing should be done or at least on a scale at which compaction and boundary effects will not occur. Full scale physical testing can help develop a field construction procedure, determine the best material to make RFS from, and explore methods to ensure uniform compaction.

2. Naturally occurring tree root geometries should be investigated by numerical modeling and physical testing to determine if RFS with more accurate tree root geometries are better performing.

3. More numerical models ran with various soil types, root geometries and RFS material types will improve the confidence of these models being predictive. The ultimate goal of these numerical models is to develop one model that can be used to provide the best RFS for the engineering problem at hand.

REFERENCES

AASHTO. 2016. "2017 Interim Revisions to the LRFP Specifications for Structural Supports for Highway Signs, Luminaires, and Traffic Signals." *AASHTO*, 40.

Ada County Highway District. 2018. "Standard Signal and CCTV Pole Foundation Detail, TS-1110.01." ITD.

Benyus, J. 1997a. *Biomimicry: Innovation Inspired by Nature.* New York : Morrow.

Benyus, J. M. 1997b. *Biomimicry: Innovation Inspired by Nature.* New York, USA: Harper Collins.

Benyus, J. M. 2008. "A Good Place to Settle: Biomimicry, Biophilia, and the Return of Nature's Inspiration to Architecture." *Biophilic Design: The Theory, Science and Practice of Bringing Buildings to Life.* New Jersey: John Wiley and Sons.

Büsgen, M., E. Munch, and T. Thompson. 1929. *The structure and Life of Forest Trees.* London: Chapman and Hall.

Coder, K. 2018. *Tree Anchorage & Strength Manual.* Manual. Warnell School of Forestry & Natural Resources, University of Georgia, Thompson Mills Forest & State Arboretum Outreach Product.

Dobson, M. 1995a. "Tree Root Systems." *Arboriculture Research and Information Note.*

Dobson, M. 1995b. *Tree Root Systems.* Arboriculture Research and Information Note. Research Note. Farnham: Arboriculture Advisory and Information Service.

Ennos, A. R. 1993. "The Scaling of Root Anchorage." *Journal of Theoretical Biology,* 161 (1): 61–75. https://doi.org/10.1006/jtbi.1993.1040.

Fouad, F. H., and E. Calvert. 2003. "Wind Load Provisions in 2001 AASHTO Supports Specifications." *Transportation Research Record,* 1845 (1): 10–18. https://doi.org/10.3141/1845-02.

Helms, M., S. Vattam, and A. K. Goel. 2009. "Biologically Inspired Design: Process and Products."." *Design Studies*, 30 (5): 606–622.

Idaho Transportation Department (ITD). 2017. "Standard Drawing Light Pole Foundation Details, 619-1." ITD.

Kamchoom, V., A. Leung, and C. W. W. Ng. 2016a. "A New Artificial Root System to Simulate the Effects of Transpiration-Induced Suction and Root Reinforcement." *Japanese Geotechnical Society Special Publication*.

Kamchoom, V., A. Leung, and C. W. W. Ng. 2016b. "A new artificial root system to simulate the effects of transpiration-induced suction and root reinforcement." *Japanese Geotechnical Society Special Publication*, 2: 236–240. https://doi.org/10.3208/jgssp.HKG-22.

Liang, T., J. A. Knappett, A. G. Bengough, and Y. X. Ke. 2017. "Small-Scale Modelling of Plant Root Systems Using 3D Priting, with Applications to Investigate the Role of Vegetation on Earthquake-Induced Landslides." *Springerlink.com*.

Mak, T. W., and L. H. Shu. 2004. "Abstraction of Biological Analogies for Design." *CIRP Annals-Manufacturing Technology,* 53 (1): 117–120.

Martinez, A., J. Dejong, I. Akin, C. Arson, J. Atkinson, P. Bandini, T. Baser, R. Borela, R. Boulanger, M. Burrall, Y. Chen, C. Collins, D. Cortes, S. Dai, T. DeJong, E. Del Dottore, K. Dorgan, R. Fragaszy, J. Frost, and J. Zheng. 2021. "Bio-inspired geotechnical engineering principles, current work, opportunities and challenges." *Géotechnique*. https://doi.org/10.1680/jgeot.20.P.170.

National Park Service. 2007. "NPS: The Giant Sequoias of California (Size of the Giant Sequoia)." Accessed August 1, 2022. https://www.nps.gov/parkhistory/online_books/cook/sec5.htm.

Rahardjo, H., F. R. Harnas, E. C. Leong, P. Y. Tan, Y. K. Fong, and E. K. Sim. 2009. "Tree stability in an improved soil to withstand wind loading." *Urban Forestry & Urban Greening*, 8 (4): 237–247. https://doi.org/10.1016/j.ufug.2009.07.001.

Raju Aedla, E. 2014. "Bio-Inspired Solutions for Durable Concrete." *International Journal of Earth Science and Engineering*.

Rodriguez, C. M., M. A. Pando, M. Whelan, D. Weggel, and H. Fang. 2020. *State of Practice and Literature Review on Foundations for Coastal Traffic Signal Mast Arm Structures.* North Carolina Department of Transportation.

Setunge, S., N. Nguyen, B. Alexander, and L. Dutton. 2009. "Leaching of Alkali from Concrete in Contact with Waterways." *Water, Air, & Soil Pollution: Focus*, 9: 381–391. https://doi.org/10.1007/s11267-009-9234-x.

Shrestha, S., and N. Ravichandran. 2020. "An Effort to Develop a Novel Foundation through Biomimicry Using 3D Finite Element Modeling." *Geo-Congress 2020*, 209–218. Geo-Congress.

Shruti. 2019. "Root System of Palm Trees." Accessed October 7, 2021. https://studiousguy.com/root-system-palm-trees/.

Stachew, E., T. Houette, and P. Gruber. 2021. "Root Systems Research for Bioinspired Resilient Design: A Concept Framework for Foundation and Coastal Engineering." *Frontiers in Robotics and AI*, 8: 109. https://doi.org/10.3389/frobt.2021.548444.

Stokes, A., and D. Guitard. 1997a. *Biology of Root Formation and Development*. Springer US.

Stokes, A., and D. Guitard. 1997b. "Tree Root Response to Mechanical Stress." *Biology of Root Formation and Development*, A. Altman and Y. Waisel, eds., 227–236. Boston, MA: Springer US.

"The Biomimicry Institute." 2020. *Biomimicry Institute*. Accessed October 7, 2021. https://biomimicry.org/.

Thiyyakkandi, S., M. McVay, P. Lai, and R. Herrera. 2016. "Full-scale coupled torsion and lateral response of mast arm drilled shaft foundations." *Canadian Geotechnical Journal*, 53 (12): 1928–1938. https://doi.org/10.1139/cgj-2016-0241.

Tobin, B., J. Cermák, D. Chiatante, F. Danjon, A. Di Iorio, L. Dupuy, A. Eshel, C. Jourdan, T. Kalliokoski, R. Laiho, N. Nadezhdina, B. Nicoll, L. Pagès, J. Silva, and I. Spanos. 2007. "Towards developmental modelling of tree root systems." *Plant Biosystems*, 141: 481–501. https://doi.org/10.1080/11263500701626283.

UN Climate Change News. 2018. "World Cement Association Urges Climate Action." 2018.

UN Environmental Program. 2020. "Building sector emissions hit record high, but low-carbon pandemic recovery can help transform sector – UN report." https://www.unep.org/news-and-stories/press-release/building-sector-emissions-hit-record-high-low-carbon-pandemic.

Vaile, E., and M. McKnight. 2017. "Sabal palmetto - Palmpedia - Palm Grower's Guide." Accessed May 31, 2021. https://www.palmpedia.net/wiki/Sabal_palmetto.

Welker's Grove Nursey. 2021. "GiantSequoia.com."

Zhang, Z., X. Wang, J. Tong, and C. Stephen. 2018. "Innovative Design and Performance Evaluation of Bionic Imprinting Toothed Wheel." *Applied Bionics and Biomechanics*, 2018: 1–11. https://doi.org/10.1155/2018/9806287.